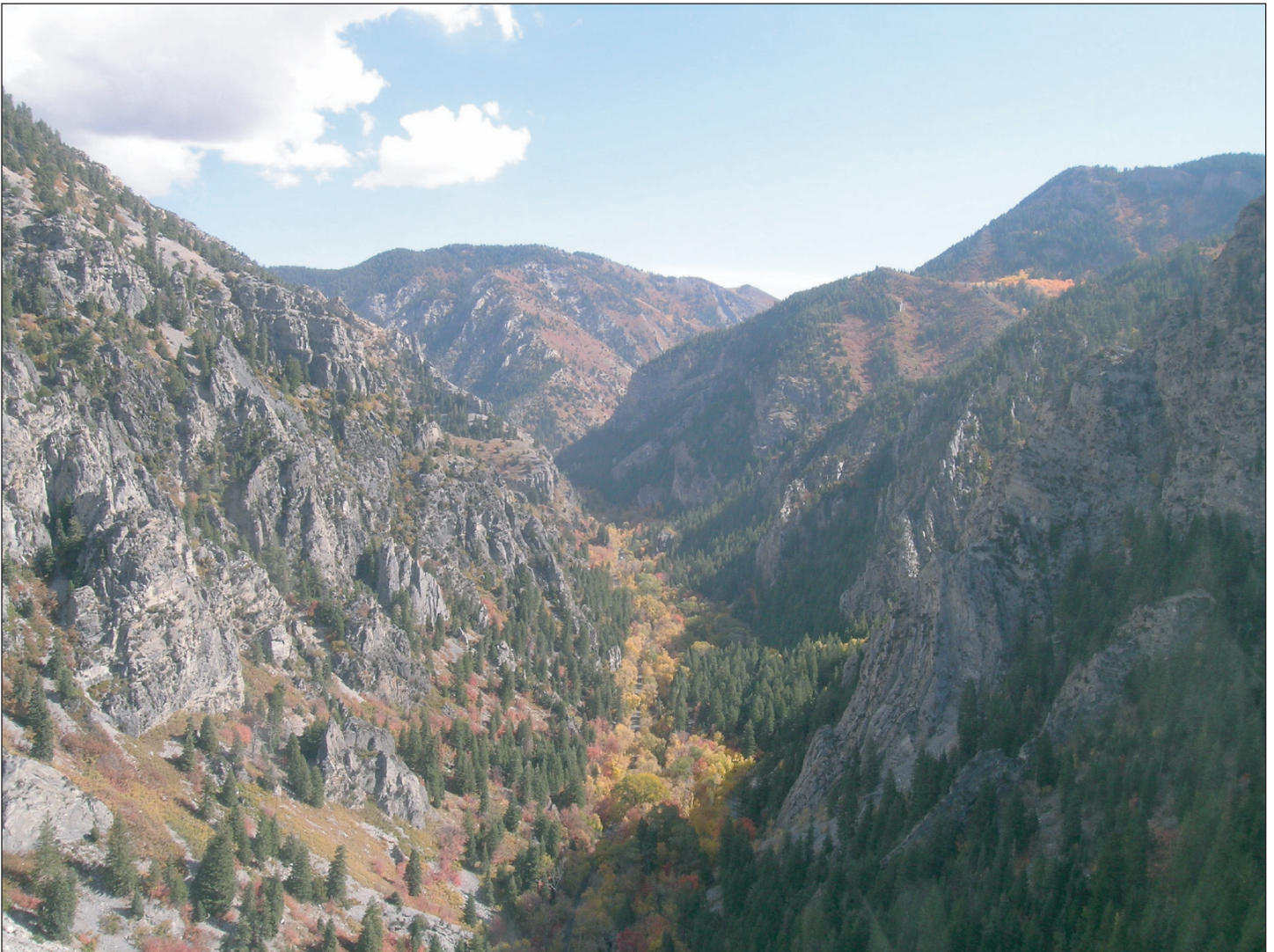




Prepared in cooperation with the Pleasant Grove District, Uinta National Forest

Rock-Fall Hazard Assessment of Little Mill Campground, American Fork Canyon, Uinta National Forest, Utah

By Jeffrey A. Coe, Edwin L. Harp, Arthur C. Tarr, and John A. Michael



U.S. Geological Survey Open-File Report 2005–1229

**U.S. Department of the Interior
U.S. Geological Survey**

U.S. Department of the Interior

Gale A. Norton, Secretary

U.S. Geological Survey

Charles G. Groat, Director

U.S. Geological Survey, Reston, Virginia 2005

Revised and reprinted: 2005

For product and ordering information:

World Wide Web: <http://www.usgs.gov/pubprod>

Telephone: 1-888-ASK-USGS

For more information on the USGS—the Federal source for science about the Earth, its natural and living resources, natural hazards, and the environment:

World Wide Web: <http://www.usgs.gov>

Telephone: 1-888-ASK-USGS

Although this report is in the public domain, permission must be secured from the individual copyright owners to reproduce any copyrighted material contained within this report.

This report has not been reviewed for stratigraphic nomenclature.

Any use of trade, firm, or product names is for descriptive purposes only and does not imply endorsement by the U.S. Government.

COVER PHOTO: Overview of American Fork Canyon and Little Mill campground. View is to the east. Little Mill campground is along the right (south) side of the canyon floor.

Rock-Fall Hazard Assessment of Little Mill Campground, American Fork Canyon, Uinta National Forest, Utah

By Jeffrey A. Coe, Edwin L. Harp, Arthur C. Tarr, and John A. Michael

Abstract

American Fork Canyon is a dramatic, deeply incised canyon that transects the Wasatch Mountain Range northeast of the town of American Fork in central Utah. Little Mill campground is located along the south side of the canyon floor just west of the South Fork Ranger station. Our assessment of rock-fall hazard at the campground indicates that all campsites are exposed to hazards from falling rocks. The hazard is highest near the flanks of the canyon floor and lowest in the center of the canyon floor. Rock-mass-quality measurements, information on historical rock falls, and engineering-geologic mapping indicate that rock-fall susceptibility is correlated with the degree of tectonic deformation (folding) of cliff forming, limestone bedrock. Tightly folded, steeply dipping bedrock is very susceptible to rock-fall initiation whereas broadly folded, gently dipping bedrock is moderately susceptible to rock-fall initiation. Rock-fall travel paths downslope from cliffs are identified as primary (paths with a high frequency of rock falls) or secondary (paths with a moderate frequency of rock falls) based on the freshness of talus, degree of soil development, maturity of vegetation, and historical scars on trees and asphalt pavement. Of the 79 campsites, 31 sites are downslope from very high or high rock-fall susceptibility areas, with 26 of these sites located downslope from primary travel paths. Forty-one campsites are downslope from moderate susceptibility areas, with 20 of these located downslope from primary travel paths. Seven campsites are located around the periphery of large debris fans, and thus have a low rock-fall hazard rating. Measurements of rock travel distances of previous rock falls in and near the campground indicate that, of the rocks that travel past the footslope (the break in slope at the north and south edges of the canyon floor), about 52 percent go beyond 10 meters, 11 percent go beyond 20 meters, and 4 percent go beyond 30 meters. Of the 72 campsites that are located downslope from moderate to very high susceptibility areas, 41 are less than 10 meters from the footslope, 14 are between 10 and 20 meters from the footslope, 10 are between 20 and 30 meters, and 7 are greater than 30 meters from the footslope. Rock-fall modeling would improve estimates of rock-fall motion and runout at specific campsites and constrain the design of possible mitigation schemes.

Introduction

In July 2004, at the request of Pam Gardner, District Ranger for the Pleasant Grove District of the Uinta National Forest,

Ed Harp of the U.S. Geological Survey (USGS) conducted a preliminary assessment of the rock-fall hazard at Little Mill campground in American Fork Canyon, Utah (fig. 1; Ed Harp, written commun., 2004). The campground has had a history of rock-fall activity (2001 U.S. Forest Service Safety Committee report provided by Pam Gardner, written commun., 2004) and lies immediately east of a former U.S. Forest Service (USFS) picnic site (Hanging Rock picnic area, fig. 1B and fig. 2) where two people were killed by separate rock-fall incidents in the mid-1990s. Harp's preliminary assessment of rock-fall hazard at the campground indicated that parts of the campground were located immediately downslope from active talus chutes and that rock from some previous falls had traveled through the campground and across the adjacent American Fork River (fig. 1C). Harp concluded his preliminary assessment with the recommendation that a detailed assessment of rock-fall hazard at the campground be conducted by using a combination of field- and aerial-based methods. The USFS funded the USGS to conduct this detailed hazard assessment in October and November 2004. This report describes the methodology, results, and conclusions from the detailed hazard assessment.

Physiographic and Geologic Setting of American Fork Canyon

American Fork Canyon is a dramatic, deeply incised canyon that transects the Wasatch Mountain Range northeast of the town of American Fork in central Utah (fig. 1A).

The lower part of the canyon, including the reach containing Little Mill campground, is V-shaped and has been carved by downcutting of the American Fork River. The upper part of the canyon above Tibble Fork (fig. 1A) was glaciated in Pleistocene time (Baker and Crittenden, 1961). The upper parts of several tributaries of the American Fork River also were glaciated. These include Rock Canyon, Little Mill Canyon, and South Fork (fig. 1A). The area is characterized by high to extreme relief. Average relief between Mount Timpanogos, which lies south of American Fork Canyon, and the base of the range near Pleasant Grove, is about 380 m/km (fig. 1A). Relief perpendicular to American Fork Canyon at Little Mill campground ranges from 550 to 850 m/km (fig. 1B).

The Wasatch Range is tectonically active. The western flank of the range forms the eastern boundary of the Basin and Range province of western North America. This boundary is marked by a zone of active earthquake faults known as the Wasatch fault

1A

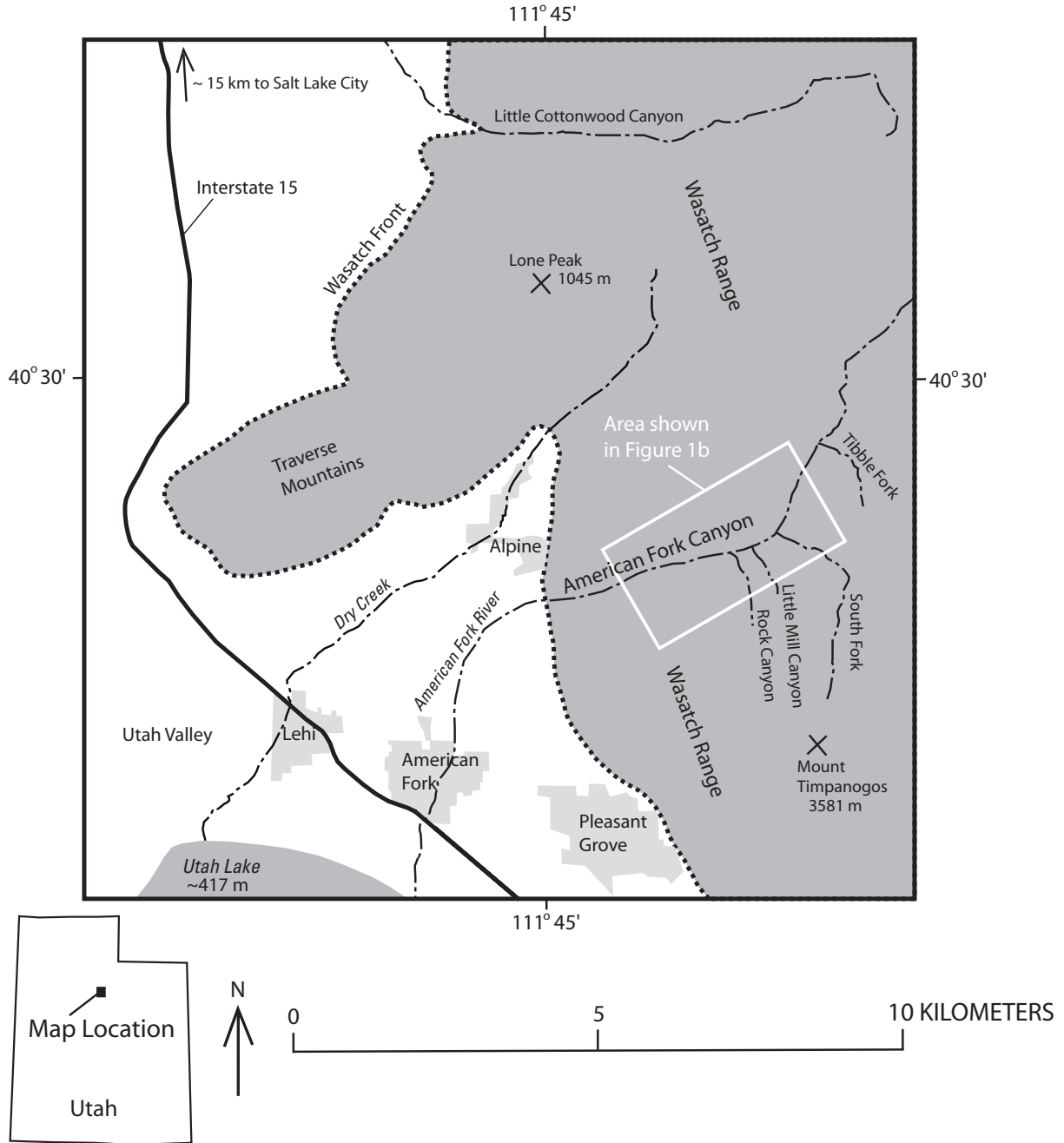
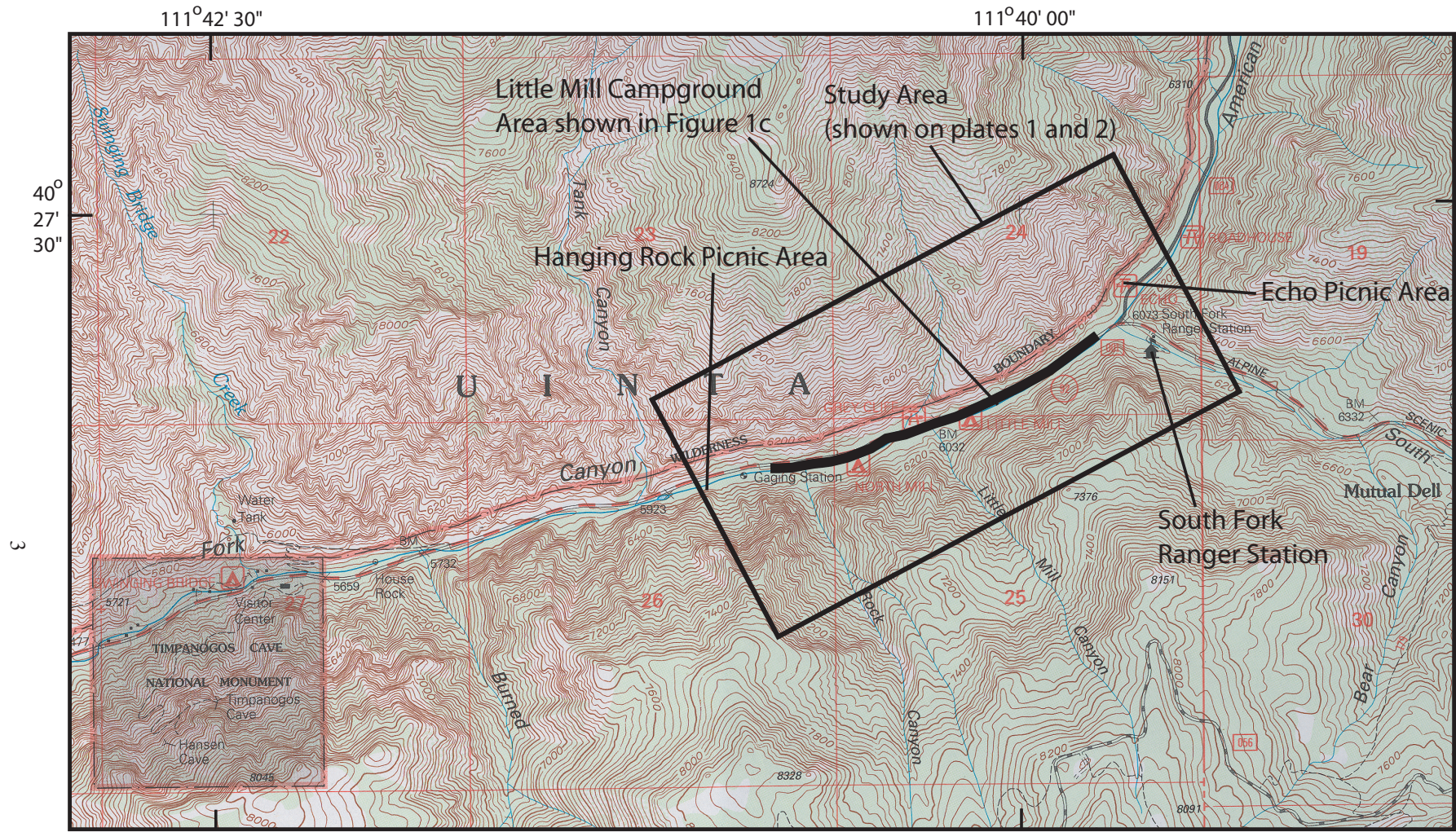


Figure 1. Maps showing location of American Fork Canyon and Little Mill campground. (A) Regional location map showing American Fork Canyon with respect to the Wasatch Front. Light gray shaded areas are towns. (B) USGS topographic map showing the location of Little Mill campground in American Fork Canyon. (C) Map showing individual campsites in Little Mill campground.



Base map is a part of the U.S. Geological Survey, Timpanogos Cave, Utah, 1:24000-scale quadrangle. North American Datum of 1927. Contour interval is 40 feet. National Geodetic Vertical Datum of 1929.



Figure 1. Maps showing location of American Fork Canyon and Little Mill campground. (A) Regional location map showing American Fork Canyon with respect to the Wasatch Front. Light gray shaded areas are towns. (B) USGS topographic map showing the location of Little Mill campground in American Fork Canyon. (C) Map showing individual campsites in Little Mill campground—Continued.

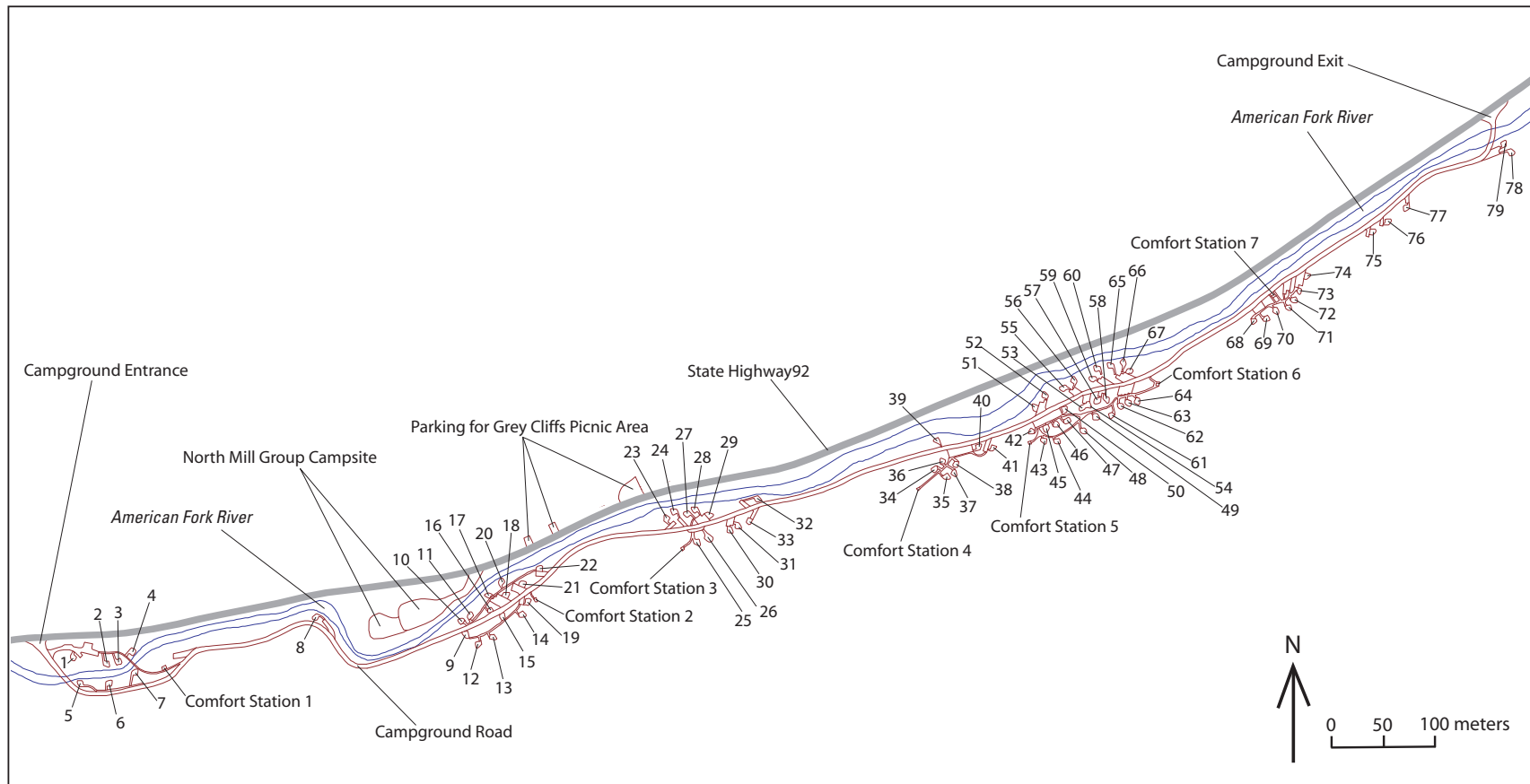


Figure 1. Maps showing location of American Fork Canyon and Little Mill campground. (A) Regional location map showing American Fork Canyon with respect to the Wasatch Front. Light gray shaded areas are towns. (B) USGS topographic map showing the location of Little Mill campground in American Fork Canyon. (C) Map showing individual campsites in Little Mill campground—Continued.



A

Figure 2. Limestone cliff at the now abandoned Hanging Rock picnic area. See Figure 1B for location. (A) View from the ground. Photograph taken on October 24, 2004. (B) View of the upper part of the limestone cliff from the opposite (north) side of the canyon. Photograph taken on October 26, 2004.



B

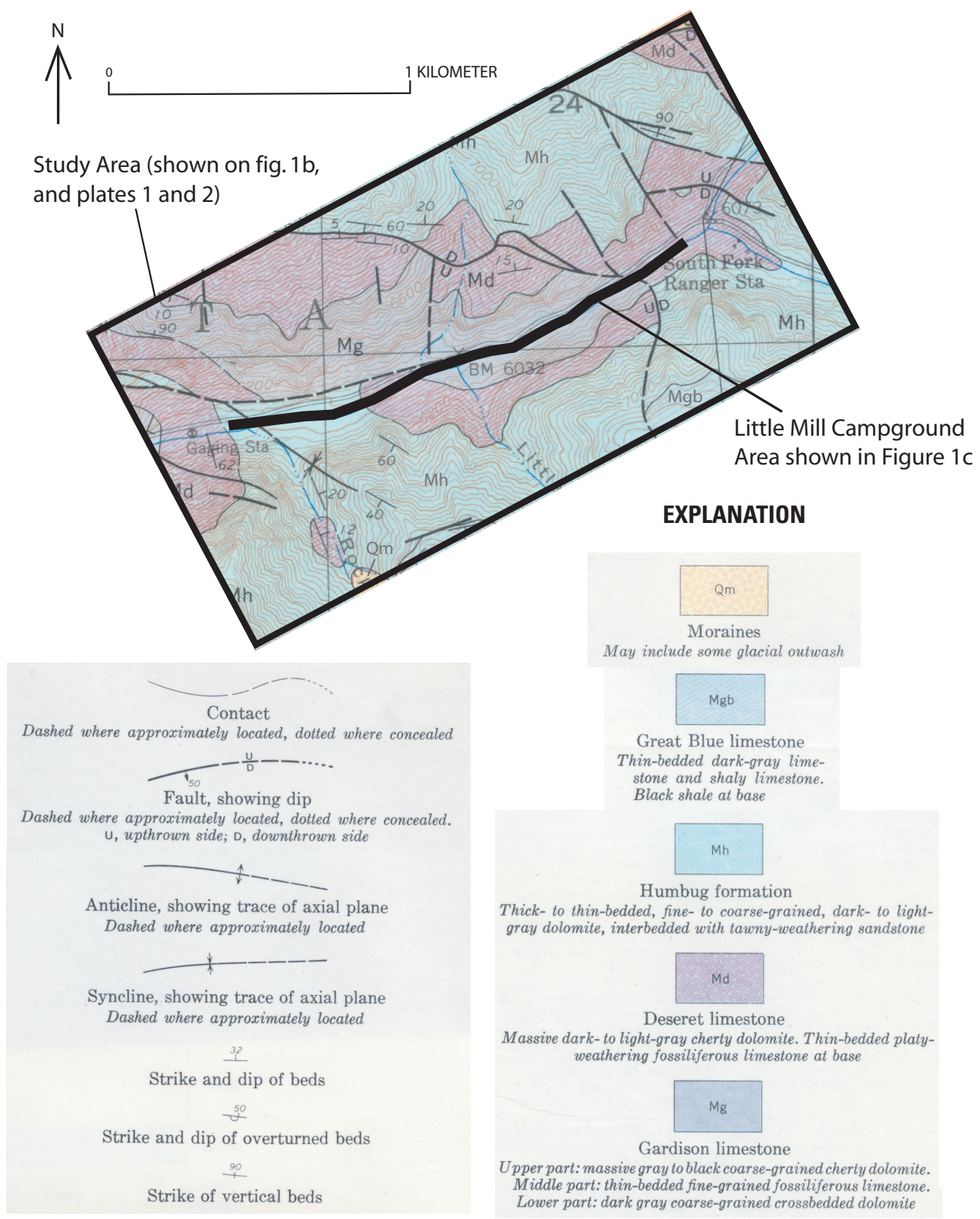


Figure 3. Geologic map of the area surrounding Little Mill campground. Modified from Baker and Crittenden (1961).



Figure 4. U-shaped fold (a syncline) with steeply dipping limbs above the west end (entrance) of the campground. Campground entrance station is visible at the bottom center of the photograph. Photograph taken on October 26, 2004. View is to the southeast.



Figure 5. Photograph composite showing broadly folded rocks with shallow-dipping limbs above the central and eastern parts of the campground. Photograph taken on October 26, 2004.

zone. The surface expression of this zone is a series of prominent fault scarps which trend north-south along the steep western flank of the range. The average recurrence interval between surface-rupturing earthquakes in the central part of the fault zone, including the area near the mouth of American Fork Canyon is about 400 years (Machette and others, 1992).

Older faults and folds within the Wasatch range are exposed in American Fork Canyon. Several of these older features are present in the vicinity of Little Mill campground (fig. 3). The most prominent of these features are a series of folds with axes that are acute to perpendicular to the direction of the canyon. In general, these folds have steeply dipping limbs near the west end of the campground (fig. 4) and shallow to moderately dipping limbs near the center and east end of the campground (fig. 5). The folds deform a thick sequence of limestones of Mississippian age (fig. 3). These limestones are divided into four formations (Baker and Crittenden, 1961), the Gardison Limestone, Deseret Limestone, Humbug Formation, and the Great Blue limestone (listed from oldest to youngest). The Gardison is a series of interbedded, fine- to coarse-grained limestones and dolomites. The Deseret primarily is a massive dolomite with a thin-bedded limestone near the base. The Humbug is composed of an alternating series of limey sandstones and thin-to thick-bedded limestones and dolomites. The Great Blue limestone is a thinly-bedded limestone and shaly limestone with black shale near the base of the unit. Most rocks immediately adjacent to Little Mill are in the Gardison, Deseret, and Humbug Formations (fig. 3).

Methods

The three components of many rock-fall hazard assessments (Mazzocola and Sciesa, 2000; Guzzetti and others, 2003; Dorren, 2003) are a determination of the relative susceptibility of rock outcrops to rock-fall initiation, identification of travel paths of potential rock falls, and an estimation of the travel distance of rock falls (here after referred to as rock-fall *runout*). To address these components, we used an approach that included five methods—helicopter reconnaissance, a compilation of historical rock falls, field observations and large-scale geologic mapping, rock-mass quality measurements, and rock-fall runout

measurements. The hazard components that each of these methods addressed are given in table 1. A description of each method is given below.

Helicopter Reconnaissance

On October 5, 2004, the cliffs above the campground on both sides of the canyon were inspected visually using a helicopter provided by the USFS. The inspection consisted of multiple passes over the campground at various altitudes. This reconnaissance provided visual access to portions of cliffs that are difficult to see from the ground.

Compilation of Historical Rock Falls

We compiled information on historical rock falls in and near Little Mill campground using newspaper articles, eyewitness accounts, personal observations, and published reports. We searched the online archive of the *Deseret News* newspaper for articles that described rock falls using the keywords “rock fall”, “rockfall”, “rock slide”, “rockslide”, “falling rock”, “American Fork Canyon”, “Little Mill campground”, “Highway 92”, and “U-92”. The online archive included articles from 1988 to 2005. Eyewitness accounts were provided by Melissa Crumpton, John Hendrix, Dean Larsen, and Larry Velarde, all of the Pleasant Grove District of the Uinta National Forest. Personal observations were made by the authors in October and November 2004. The record of historical rock falls documented in this report is incomplete because newspaper articles prior to 1988 were not systematically searched, and because there clearly have been historical rock falls that have not been observed or recorded in any newspaper or report.

Field Observations and Geologic Mapping

Field observations and geologic mapping were conducted as an iterative process. Observations initially were made during trips to the field in July and early October 2004. These observations included identifying source areas for recent rock falls, recording the degree of deformation (folding) of rocks in source areas, noting the freshness of talus deposits, and identifying the

Table 1. Methods used to address each rock-fall hazard component.

Component of rock-fall hazard	Methods used to address
Susceptibility to rock-fall initiation	Helicopter reconnaissance, compilation of historical rock-falls, field observations and geologic mapping, rock-mass quality measurements
Identification of rock-fall travel paths	Helicopter reconnaissance, compilation of historical rock-falls, field observations and geologic mapping
Estimation of rock-fall runout	Compilation of historical rock-falls, rock-fall-runout measurements

location, type, and freshness of rock-fall scars on trees and asphalt surfaces. After these initial observations were made, we produced an engineering geologic map (pl. 1) using 1:6000-scale stereographic aerial photographs taken in 1983. To produce the map, the photographs were registered to a 1:3000-scale paper copy of a USGS Digital Orthophoto Quadrangle (DOQ) from the northeastern quarter of the Mt. Timpanogos 1:24,000-scale quadrangle. A PG-2 photogrammetric plotter (Pillmore, 1989) was used to register the photographs. Once registered, geologic contacts were transferred from the photographs to the 1:3000-scale paper and digitized into the ArcInfo Geographic Information System (GIS). The digitized geologic map then was taken to the field during additional trips in late October and early November 2004. During these trips, the map was checked for completeness and accuracy, and revisions were made.

Additional features shown on the engineering geologic map (pl. 1) include the American Fork River, Highway 92, 40 ft. contour lines, the campground road, campground parking areas, and individual campsites. The river, Highway 92, the campground road, and parking areas were transferred from the 1983 photographs using the PG-2 plotter. Contour lines are from USGS Digital Line Graph data of the Mt. Timpanogos quadrangle. The original intended scale of these contours is 1:24,000. Our map is presented at 1:3,000-scale. At 1:3,000-scale, the contour lines can be viewed only as a general indicator of topographic conditions, and not as a highly accurate representation of topographic details. In several areas where the contours obviously were incorrect at 1:3000-scale, we edited the lines to fit our field and aerial photograph observations. Contours that have been edited are dashed on the map. Individual campsites were derived from a 1:600 scale, as-built, architectural drawing provided by Bernadette Berthalengi, a landscape architect with in the USFS Provo, Utah, office. Registering this information to the geologic map was difficult and inexact. The campsites were digitized into ArcInfo and then locally fit to the campground road and parking areas that were transferred from the 1983 aerial photographs. Our best estimate is that the location of individual campsites shown on plates 1 and 2 could be different from their actual locations by several meters.

Rock-Mass Quality

To assess the relative rock-fall susceptibility of cliffs above the campground, we used an engineering rock-classification scheme known as Rock-Mass Quality (Barton and others, 1974; Harp and Noble, 1993). This classification scheme uses the characteristics of rock discontinuities (joint, fracture, and bedding planes) to quantify the potential for failure (rock-fall initiation). Rock Mass Quality (Q) is determined using numerical ratings for six discontinuity characteristics as measured in a cubic meter of rock at various field sites. Values of Q are calculated using the equation

$$Q = \left[\frac{115 - 3.3J_v}{J_n} \right] \left[\frac{J_r}{J_a} \right] \left[\frac{J_w}{AF} \right], \quad \text{Equation 1}$$

where J_v is the total number of discontinuities, J_r is the roughness of the surface of the discontinuities, J_n is the number of sets of discontinuities, J_a is the type of filling or alteration on the surface of discontinuities, J_w is the water reduction factor, and AF is the aperture or “openness” of discontinuities. The expression $115 - 3.3J_v$ also is known as Rock Quality Designation (Deere and Deere, 1989; Palmström, 1982). Numerical ratings for each of these factors are assigned based on the correlation of field measurements and observations with descriptive rankings (Harp and Noble, 1993). The rankings used in this study are shown in table 2. In our application, that is, surficial measurements with mostly dry discontinuities, the J_w value in the third quotient is equal to 1.0 (Harp and Noble, 1993). Values of Q are inversely related to susceptibility. That is, as Q decreases, rock-fall susceptibility increases.

We made measurements of discontinuity characteristics at 72 field sites (pl. 1) in October and November 2004. Thirty-six sites were on the south side of the canyon, and 36 were on the north side of the canyon (pl. 1). Discontinuities were dry when we made our measurements. During wetter times of the year, when water may be present in the discontinuities, the values of Q derived from our measurements would be lower depending on the amount of water present (see J_w in table 2).

Various other factors in equation 1 were used to estimate other properties of the measured rock mass. The first quotient, $(115 - 3.3J_v)/J_n$, approximates the relative block size of the mass (Barton and others, 1974). For example, if one site has a relative block size of 4, and another has a relative block size of 1, then blocks at the first site are 4 times larger than blocks at the second site. In addition to estimates of block size made using this relative index, we also estimated an absolute average block volume (V_b) and block edge size (S_b) using a method described by Palmström (1995). This method uses the parameter J_v in the equation:

$$V_b = \beta * J_v^3, \quad \text{Equation 2}$$

where β is a block shape factor that is defined or estimated based on the spacing of discontinuities. According to Palmström (1995), rock masses containing three or more sets of discontinuities, as is the case at Little Mill, typically form equidimensional cubes or moderately long, flat blocks with β values that range from 27 to 75. Our field observations from Little Mill indicate that blocks in historical rock falls and in talus deposits typically are equidimensional to moderately flat and elongated. Therefore, in our calculation of V_b , we used a β value of 50 to estimate the average V_b . The average block edge size (S_b) was estimated by $\sqrt[3]{V_b}$. An inherent assumption in equation 2 is that all sets of discontinuities intersect one another at 90° angles (Palmström, 1995). At Little Mill, some discontinuities intersect at 90° angles, whereas others intersect at angles other than 90°. Therefore, the V_b values calculated from equation 2, as well as the S_b values, should be considered minimums.

Table 2. Ratings used for Rock Mass Quality parameters given in equation 1. Note that we interpret “Joint” to be synonymous with “discontinuity”, which is used throughout the text. From Barton and others (1974) and Harp and Noble (1993).

Rating used in Equation 1
↓

1. Total Number of Joints per Cubic Meter (J_v)	Note: (i) When the term $(115 - 3.3J_v)$, known as Rock Quality Designation (RQD), is ≤ 10 (including 0), a nominal value of 10 is substituted for $(115 - 3.3J_v)$ in Equation 1.
2. Joint Set Number (J_n) A. Massive, no or few joints 0.5–1.0 B. One joint set 2 C. One joint set plus random 3 D. Two joint sets 4 E. Two joint sets plus random 6 F. Three joint sets 9 G. Three joint sets plus random 12 H. Four or more joints sets, random, heavily jointed, “sugar cube,” etc. 15 I. Crushed rock, earthlike 20	Note: (i) For intersections $(3.0 \times J_n)$.
3. Joint Roughness Number (J_r) (a) Rock wall contact and (b) Rock wall contact before 10 cm shear A. Discontinuous joints 4 B. Rough or irregular, undulating 3 C. Smooth, undulating 2 D. Slickensided, undulating 1.5 E. Rough or irregular, planar 1.5 F. Smooth, planar 1.0 G. Slickensided, planar 0.5 (c) No rock wall contact when sheared H. Zone containing clay minerals thick enough to prevent rock wall contact 1.0 (nominal) J. Sandy, gravelly or crushed zone thick enough to prevent rock wall contact 1.0 (nominal)	Notes: (i) Add 1.0 if the mean spacing of the relevant joint set is greater than 3 m. (ii) $J_r = 0.5$ can be used for planar slickensided joints having lineations, provided the lineations are favorably orientated.
4. Joint Alteration Number (J_a) (a) Rock wall contact A. Tightly healed, hard, non-softening, impermeable filling, i.e. quartz or epidote 0.75 B. Unaltered joint walls, surface only 1.0 C. Slightly altered joint walls. Nonssoftening mineral coatings, sandy particles, clay-free disintegrated rock, etc. 2.0 D. Silty- or sandy-clay coatings, small clay-fraction (non-softening) 3.0 E. Softening or low-friction clay mineral coatings, i.e. kaolinite, mica. Also chlorite, talc, gypsum and graphite, etc., and small quantities of swelling clays. (Discontinuous coatings, 1–2 mm or less in thickness) 4.0	
5. JOINT WATER REDUCTION FACTOR (J_w) A. Dry excavations or minor inflow, i. e. < 5 l/min. locally 1.0 B. Medium inflow or pressure occasional outwash of joint fillings 0.66 C. Large inflow or high pressure in competent rock with unfilled joints 0.5 D. Large inflow or high pressure, considerable outwash of joint fillings 0.33 E. Exceptionally high inflow or water pressure at blasting, decaying with time 0.2–0.1 F. Exceptionally high inflow or water pressure continuing without noticeable decay 0.1–0.0	
6. Aperture (A_f) A. All joints tight 1.0 B. Most joints tight, a few open as much as 2 cm 2.5 C. Most joints tight, a few loose, open as much as 5 cm 5.0 D. Significantly (20 percent) open, as much as 10 cm 7.5 E. Greatly (60 percent) open, as much as 20 cm 10.0 F. Gaping open, many joints open > 20 cm 15.0	Notes: (i) If perched or loose rocks are common, increase by one. (ii) If pervasive joints dip out of slope, increase by one.

An estimate of interblock shear strength was calculated from the second quotient of equation 1, J_r/J_a . This quotient, when expressed as $\tan^{-1}(J_r/J_a)$, approximates the shear strength that might be expected for various combinations of discontinuity roughness and alteration products (Barton, and others, 1974). Barton stated that this apparent shear strength is very similar to total friction angle (combined cohesion and friction = $\tan^{-1} \tau/\sigma$, where τ = shear strength, and σ =normal stress) of the rock mass.

The third quotient in equation 1, J_w/AF , which is $1/AF$ in our application, was used to estimate the relative “tightness” of the rock at each site. High values indicate “tight” rock. Stated another way, high values indicate that rock discontinuities have smaller apertures, or are less open, than discontinuities in rocks with low values.

Rock-Fall Runout Measurements

A critical component of the hazard assessment was estimating how far future rock falls are likely to travel. Rock-fall hazard assessments in other areas have used field- and modeling-based approaches to assess rock-fall runout distances. Evans and Hungry (1993) used the angle formed between the top of talus deposits and the distal limit of rock-fall runout to estimate rock-fall runout zones or “rockfall shadows”. Guzzetti and others (2003) used a computer program (STONE, Guzzetti and others, 2002) to estimate rock-fall runout in Yosemite National Park. Wiczorek and Snyder (1999) differentiated two zones of rock-fall runout in Yosemite National Park—a zone for large boulders that rolled or bounced along slopes and a zone of small rocks that generally flew through the air (so called “fly-rock”) following impact and breakup of larger rocks along cliffs or talus deposits. At Little Mill, our options for estimating runout were somewhat limited because the available topographic information is of low resolution (40 ft contours mapped at 1:24,000 scale) compared to the map scale (1:3000) required for portraying the hazard at individual campsites. Therefore, to estimate the travel distance of future rock falls, we measured runout distances of previous rock falls. We measured two types of runout distances (fig. 6)—extreme distances of isolated individual rocks (locations designated ER on pl. 1), and the distribution of distances at clusters of rocks (locations designated DR on pl. 1). Both types of distances were measured in relation to the footslope, that is, the location where the slope breaks at the foot of the hill or canyon wall (fig. 6). The canyon floor is located between the north and south footslopes. The canyon floor is relatively flat and contains isolated rocks or clusters of rocks from rock-fall events. All distances were measured from the footslope toward the center of the canyon floor. Extreme distances were measured with a single tape measure that ran perpendicular from the footslope to the side of the rock that was farthest from the footslope. Twenty distances were measured in Little Mill campground or on the north side of Highway 92 adjacent to the campground. Six additional distances were measured at rock-fall locations in or near Timpanogos Cave National Monument several kilometers (km) to the west of the campground.

The distribution of distances at clusters of rocks were measured using three tape measurements (fig. 6). Two measurement tapes were placed parallel, 5 m apart, and extended perpendicular to the footslope. A third tape was extended perpendicular to the first two in 5 m increments. In each increment, for example, from 0 to 5 m, the number of rocks were counted and recorded. In general, rocks were counted and recorded if they were larger than roughly 5 cm in one dimension and several cm in a second dimension. Finding locations to make these measurements was difficult because the river and construction of the campground and Highway 92 had disturbed the natural distribution of rocks in many areas. We chose six measurement locations (DR on pl. 1) where such disturbance was minimal. However, even in these locations, it was difficult, and sometimes impossible, to count individual rocks once distances from the footslope were greater than 20 to 30 m. Typically, the river or a road was encountered at these distances. When rock counts were not possible, we estimated the number of rocks based on the distribution of rocks closer to the footslope. We describe this technique more fully in the Results Section.

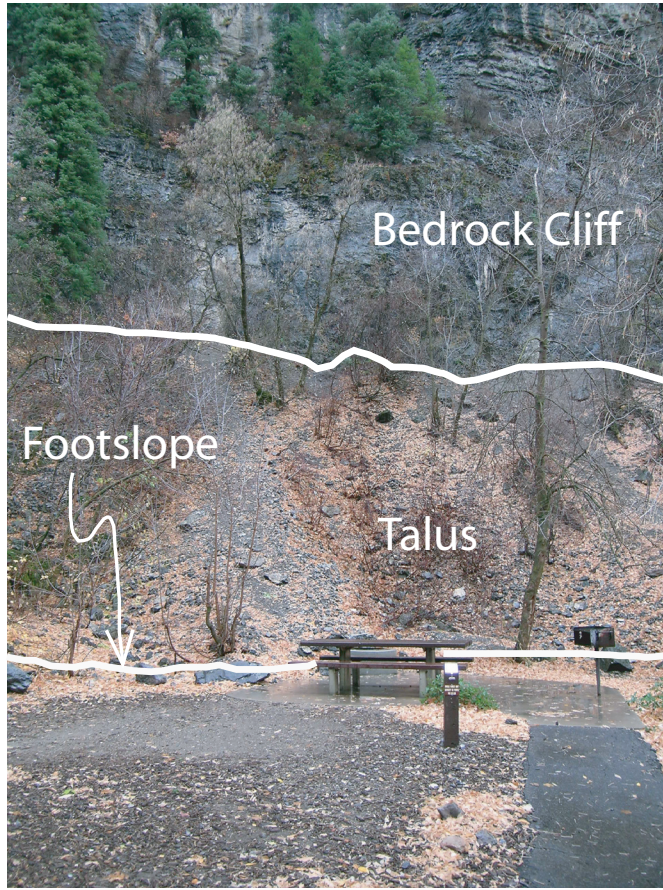
Results

Historical Rock Falls

We have compiled information on 17 historical rock falls that occurred in or immediately adjacent to Little Mill campground (figs. 7 and 8, table 3). Eight of the 17 rock falls (numbers 1, 3–6, 12, and 16–17, table 3) were concentrated between Hanging Rock picnic area and campsite 9 (see fig. 1 and pl. 1). Two of these (numbers 4 and 5) occurred in the Hanging Rock picnic area (fig. 2 and pl. 1) and resulted in two fatalities. Eight (numbers 2, 7–10, 12–15, table 3) of the other nine rock falls were scattered in areas between campsite 33 and the Echo picnic area (fig. 1 and pl. 1). The exact location of one rock fall (number 11, table 3) that injured a hiker near Little Mill is unknown.

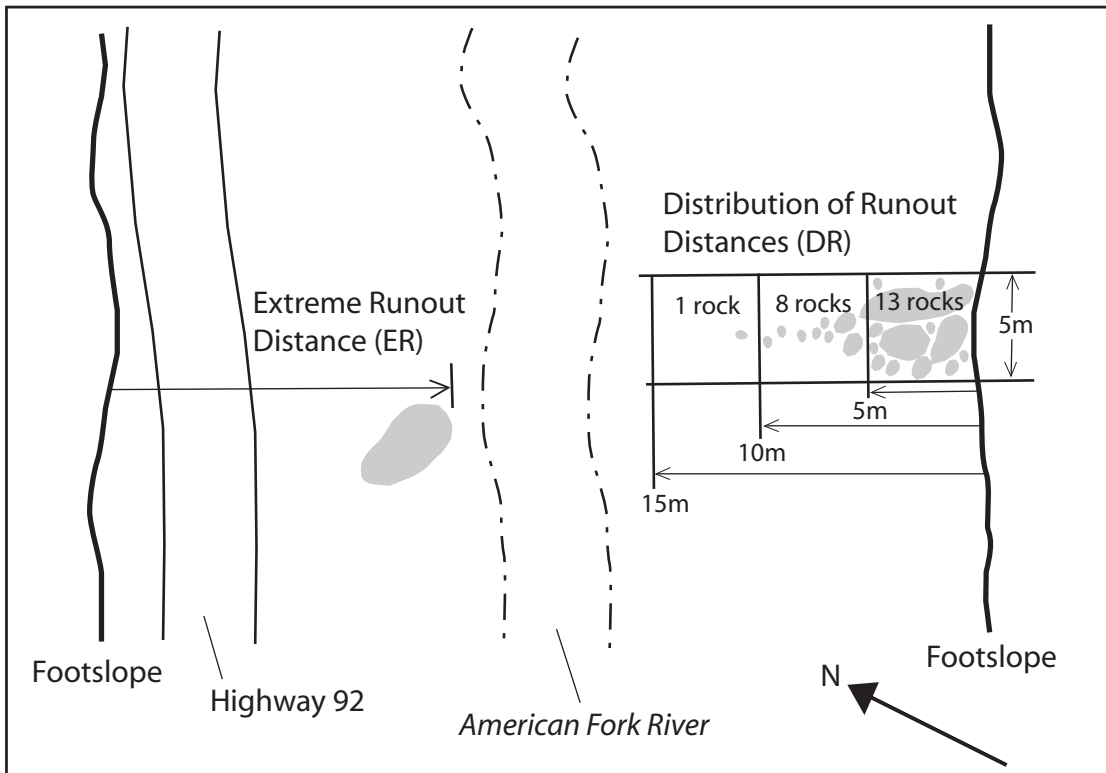
The exact times of occurrence and triggering event for most historical rock falls are not known. The times of occurrence for seven rock falls are known to within a month or better (numbers 4, 5, 11, 12, and 15–17, table 3). Of these rock falls, two occurred in July (the fatal rock falls, events 4 and 5), two in October (numbers 11 and 15), one in December (number 12), one in January (number 16), and one in April (number 17). Triggering events are known for five (numbers 4, 5, 15, 16, and 17) of the seven rock falls. The first (number 4) of the two fatal rock falls was triggered by a hiker dislodging a 25 pound rock from near the top of a cliff. The second fatality (number 5) occurred on a windy day, thus, speculation by witnesses suggested that the rock was dislodged by wind. Two rock falls (numbers 15 and 17) were triggered by several days of rainfall in October 2004 and April 2005. One rock fall (number 16) was triggered by heavy snowfall.

USFS personnel were aware of other undocumented rock falls that had to be removed from Highway 92, Highway 144, and the Little Mill campground road. Their general observation was that the most rock falls occurred during winter, during spring



A

Figure 6. Diagram showing (A) slope characteristics above campsite 48, and (B) a cartoon showing the measurement of extreme runout and the distribution of runout distances.



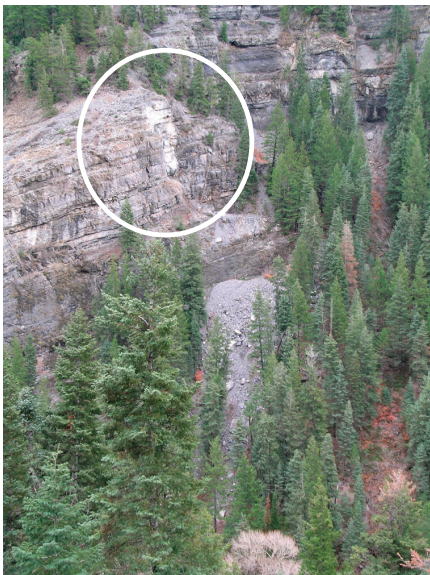
B



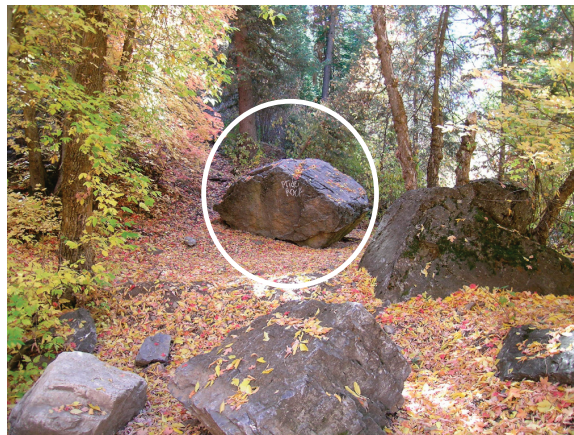
A



B



C



D



E



F

Figure 7. Pairs of photographs showing source areas (circled at left) and rocks (circled at right) from recent rock fall events described in table 3. (A, B) Rock fall 12, about 150 m west of campground entrance. (C, D) Rock fall 13 above campsite 68. (E, F) Rock fall 7 above campsite 33.



A



B



C

Figure 8. Scars in pavement from recent rock-falls (see table 3). (A) Scar (in campground road) and rock (circled) between campsite 7 and comfort station 1 (rock fall 1, table 3). (B) Scars (in campground road) and rocks (circled) near campsite 68 (rock fall 13). (C) Scar in campground road between campsites 77 and 79 (rock fall 15).

Table 3. Documented historical rock falls in and near Little Mill campground.

Rock-fall number	Location	Time and date of rock fall	Trigger	Comments	Source(s) of Information
1	Little Mill campsites 5, 6, and 7	Unspecified date to present	Unknown	Rocks from south slope repeatedly falling on campground road immediately upslope from campsites, campsites are closed for camping but used as picnic sites (for example, see fig. 8a).	2001 USFS safety committee report; personal communication with Judy Van Dyke of Mountain Campground Management and USFS employees John Hendrix, Dean Larsen, and Melissa Crumpton; field observations by authors
2	Little Mill campsite 78	Unspecified date to present	Unknown	Gradual build-up of talus from falling rocks has buried the campsite, campsite is no longer used.	2001 USFS safety committee report
3	On Highway 92 near entrance to Little Mill campground	1992 or 1993	Unknown	Rocks from north slope land on Highway 92, largest rock is the size of a Volkswagon.	Personal communication with USFS employees John Hendrix and Dean Larsen
4	Hanging Rock picnic area (fig. 2)	July 25, 1994	Rock dislodged by a hiker	California woman sitting by river, struck in head by 25 pound falling rock, dies at the scene	Deseret News, 1994; Deseret News, 1997
5	Hanging Rock picnic area (fig. 2)	~ 5:15 pm, July 29, 1995	Wind (?)	Utah teenager standing in the river, struck in head by falling rock, dies at hospital	Deseret News, 1995

Table 3. Documented historical rock falls in and near Little Mill campground.—Continued

Rock-fall number	Location	Time and date of rock fall	Trigger	Comments	Source(s) of Information
6	Little Mill campsite 3	Late 1990s	Unknown	Falling rock from south slope, impacts campground road, hits asphalt trail by restroom 1, deflects off another rock, travels across the river and lands by a tent in campsite 3.	2001 USFS safety committee report
7	Little Mill campsite 33	~1999	Unknown	Falling rock (about 0.5 x 0.5 x 0.5 m in size) from south slope hits grill at campsite, campsite is closed to camping and picnicking (see figs. 7e and 7f)	2001 USFS safety committee report
8	Outbuildings at South Fork Ranger Station	Late 1990s, early 2000s	Unknown	Boulders from rock-falls remain behind buildings and on top of a trash can.	Personal communication with USFS employees Melissa Crumpton, John Hendrix, and Dean Larsen
9	Little Mill campsite 69	Late 1990s early 2000s	Unknown	Falling rock from south slope lands next to picnic table at the campsite, campsite has been removed	2001 USFS safety committee report
10	Little Mill campsite 64	2000	Unknown	Falling rock from south slope goes through the roof of a parked trailer, through a cabinet, table, and trailer floor, and lands on the ground.	2001 USFS safety committee report

Table 3. Documented historical rock falls in and near Little Mill campground.—Continued

Rock-fall number	Location	Time and date of rock fall	Trigger	Comments	Source(s) of Information
11	Near Little Mill campground	~12:45 pm, October 15, 2000	Unknown	Utah woman hiking near Little Mill campground struck in head by basketball-sized falling rock, found unconscious, treated and released from hospital	Deseret News, 2000
12	About 150 m west of the entrance to Little Mill campground	December 17 or 18, 2000	Unknown	Massive rock fall including many large boulders from north slope cross and close Highway 92 (see figs 7a and 7b).	Personal communication with USFS employees John Hendrix and Dean Larsen, field observations by authors
13	Little Mill Campsite 68	Winter of 2000-2001	Unknown	Falling rocks from south slope land on campsite and on campground road near the campsite (fig. 7c), the largest rock is the size of a small car (fig. 7d), falls have previously affected this area as evidenced by patches in road (fig. 8b), campsite has been removed	2001 USFS safety committee report
14	At western-most picnic site in the Echo picnic area	2003 or 2004	Unknown	Rock from north slope lands on concrete picnic table pad.	Personal communication with USFS employee Melissa Crumpton
15	About half way between campsites 77 and 79.	Between October 24 and 27, 2004	Prolonged rainfall	Rock from south slope lands on, and crosses over, the campground road (fig. 8c) and stops in the river.	Observations by authors

Table 3. Documented historical rock falls in and near Little Mill campground.—Continued

Rock-fall number	Location	Time and date of rock fall	Trigger	Comments	Source(s) of Information
16	About 50 m west of campsite 9	Early January, 2005	Occurred after heavy snowfall	Rock from south slope lands on the campground road. Size of rock is roughly 0.5 x 0.5 x 0.5 m.	Personal communication with USFS employees Melissa Crumpton and Larry Velarde
17	About 100 m west of campsite 9	Night of April 28/29, 2005	Prolonged rainfall	Five rocks from south slope land on the campground road (3 rocks), the American Fork River (1 rock), and in North Mill Group Campsite (1 rock). Largest rock is roughly 2m x 2m x 1m.	Personal communication with USFS employees Larry Velarde and Quinn Hall.

snowmelt, and during or immediately after prolonged rainfall. This observation is similar to that made by Wieczorek and Snyder (2003) in Yosemite National Park.

Field Observations and Geologic Mapping

Field observations and geologic mapping contributed a considerable amount to our understanding and portrayal of rock-fall hazards at Little Mill (table 1). An engineering geologic map summarizing results from these two activities is shown on plate 1. Field observations indicated that deformation of the limestone cliffs upslope from the campground ranged from tight folds with steeply dipping limbs (fig. 4) to broad folds with shallow-dipping limbs (fig. 5). We identified a general positive correlation between extent of folding and the occurrence of historical rock falls and volume of fresh talus deposits downslope from rock outcrops. This observation indicates that, in general, rock falls occur more frequently from rocks with steeply dipping bedding than from rocks with shallow-dipping bedding. An exception to this observation is that shallow-dipping bedding in the axes of folds had a higher degree of rock fall activity than areas of shallow-dipping bedding on the limbs of broad folds. We noticed this correlation after inspecting the rock upslope from documented historical rock falls, rock-fall scars on trees, and scars on asphalt pavement. For example, eight (numbers 1, 3–6, 12, and 16–17) of the 17 documented historical rock falls in table 3 initiated from steeply dipping rocks, six (numbers 2, 7–9, 13, 15) initiated from moderately dipping rocks or the axial zones of folds, two (numbers 10 and 14) initiated from shallow dipping rocks, and the location of one rock fall (number 11) was unknown. Although these data seem to suggest that the numbers of rock falls are similar from steeply and moderately dipping rocks, steeply dipping rocks actually have produced more falls because historical rock fall number 1 (table 3), which is downslope from steeply dipping rocks, documents repeated rock-fall events. Examples of prominent historical rock falls are shown on figure 7. The rock fall shown on figures 7A and 7B initiated from steeply dipping rocks, the fall shown on figures 7C and 7D initiated from the axial zone of a fold, and the fall shown on figures 7E and 7F initiated from moderately dipping rocks. Examples of scars on asphalt pavement are shown on figure 8. The scar in figure 8A is downslope from steeply dipping rocks, whereas 8B and 8C are downslope from fold axial zones. Examples of scars on trees are shown on figure 9. Three of these scars (figures 9B, 9C, and 9D) were downslope from steeply dipping rocks, and two (figs. 9A and 9E) were downslope from fold-axial zones. Perhaps the best indicator of rock fall frequency is the mapped area of young talus (designated yt on pl. 1 and described below) downslope from rock outcrops. The mapped area of young talus is much greater downslope from steeply dipping rocks than it is downslope from moderate- and shallow-dipping rocks (pl. 1).

The engineering geologic map shown on plate 1 shows the location of limestone bedrock, fresh and older talus deposits, debris fans, debris cones, and alluvium deposited by the American Fork River. Almost all bedrock immediately adjacent

to the campground is limestone of the Gardison, Deseret, and Humbug Formations (fig. 3). Field observations indicated that the extent of deformation (steepness of dip) is better correlated with rock-fall frequency than the variations in limestone characteristics among these three Formations. Therefore, limestone bedrock units shown on plate 1 are distinguished on the basis of steepness of dip. Geologic units shown on plate 1 are further defined as follows.

Shallow-dipping limestone—limestone bedrock with bedding plane dips of roughly 20° or less. See fig. 10A and 10B for examples.

Moderately-dipping limestone and(or) fold axial zones—limestone bedrock with bedding plane dips between roughly 20° and 40°, or fold axial zones with bedding dips less than 20°. See figures 10C and 10D for examples.

Steeply dipping limestone—limestone bedrock with bedding plane dips that exceed roughly 40°. See figures 10E and 10F for examples.

Young talus deposits—steeply sloping, loose accumulations of fragmented, angular rocks ranging in size from pebbles to boulders. Talus deposits are located between bedrock cliffs and the footslope. These deposits are differentiated from older talus deposits by a general lack or sparseness of vegetation and the presence of extensive, freshly exposed surfaces on rock fragments. See figures 10G and 10H for examples.

Older talus, colluvium, and soil—a steeply sloping deposit containing a mixture of rock fragments and finer-grained soil material. These deposits occupy slope positions downslope and upslope from bedrock cliffs and are differentiated from younger talus deposits by the widespread presence of vegetation. See figures 10I and 10J for examples.

Debris fans—fan-shaped deposits at the mouths of ephemeral tributary drainages to the American Fork River that primarily were deposited by debris flows and water-dominated flows. Fans usually are covered by widespread, mature vegetation. See figure 10k for an example.

Debris cones—steep, cone-shaped deposits at the base of steep and small tributary gulleys to the American Fork River. Debris cones are smaller and steeper than debris fans and likely have been deposited by multiple processes including snow avalanches, rock falls, water-dominated flows, and debris flows (Selby, 1993). Cones usually are covered by vegetation. This definition departs from the American Geological Institute's (AGI) definition of debris cone (Bates and Jackson, 1987). AGI defines the term as an alluvial fan with very steep slopes, composed of thicker



A



B



C



D



E

Figure 9. Tree scars from rock falls in and near Little Mill campground. (A) Upslope from campsite 68. Photograph taken on October 6, 2004. (B) Downslope from measurement site Q41. Photograph taken October 25, 2004. (C) Between measurement sites Q57 and Q58. Photograph taken on October 26, 2004. (D) On north side of Highway 92, about 150 m east of campground entrance (rock fall 12 in table 3). Photograph taken on October 25, 2004. (E) North of campground road between campsites 77 and 79 (rock fall 15, table 3). Tree and rock are circled. Photograph taken October 27, 2004.



A



B



C



D



E



F

Figure 10. Examples of geologic units mapped in and near Little Mill. (A) Shallow-dipping limestone near Grey Cliffs picnic area. (B) Shallow-dipping limestone above campsites 34–67. (C) Axial fold zone above campsites 68 and 69. Dip of bedding is shown by solid line. (D) Moderately-dipping limestone at Grey Cliffs picnic area (middle part of photograph). (E) Steeply dipping bedrock in American Fork Canyon near the campground entrance and further west. View to the west. (F) Steeply dipping limestone above campsites 5 and 6. (G) Young talus upslope from campsites 5–7. (H) Young talus upslope from campsite 7. (I) Older talus, colluvium, and soil upslope from campsites 78 and 79. (J) Aerial view of axial fold zone, young talus, and older talus at measurement sites Q53 and Q54. (K) Debris-flow deposits on debris fan at the mouth of Little Mill Canyon. (L) Alluvium along the American Fork River.



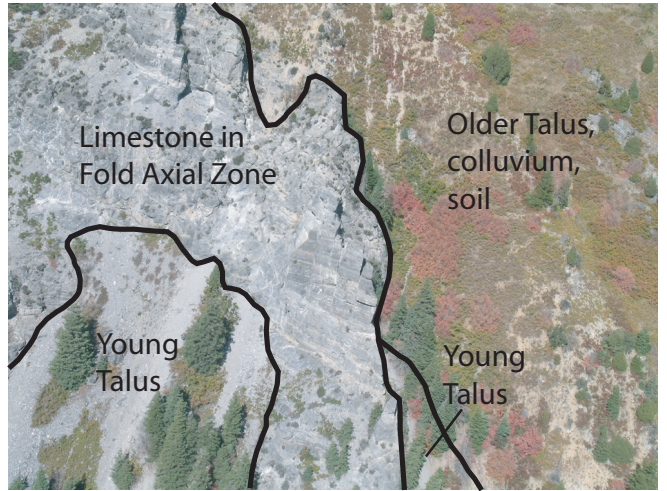
G



H



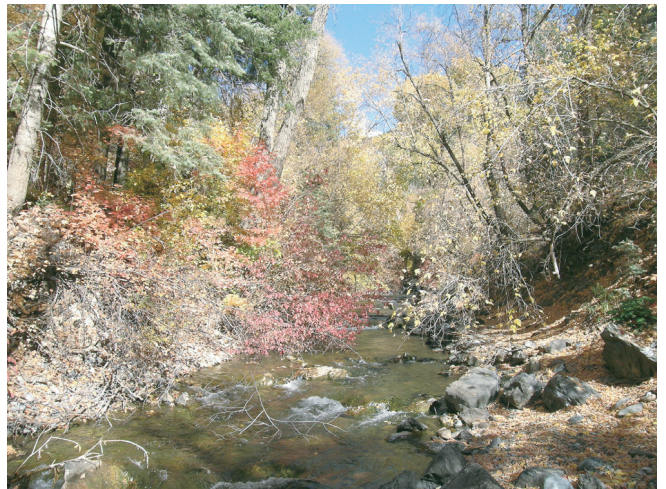
I



J



K



L

Table 4. Descriptive rankings for ranges of Q values. Barton and others (1974) studied a variety of rock types to develop the Rock Mass Quality (Q) method for mining and tunnel design. Harp and Jibson (2002) studied rock-fall susceptibility of a variety of rock types following the January 17, 1994, Northridge, California earthquake.

Range of Q values	Descriptive ranking (Barton and others, 1974)	Descriptive ranking (Harp and Jibson, 2002)
0.001–0.01	Exceptionally poor rock	Very high rock-fall susceptibility
0.01–0.1	Extremely poor rock	Very high rock-fall susceptibility
0.1–1	Very poor rock	High rock-fall susceptibility
1–4	Poor rock	Moderate rock-fall susceptibility
4–10	Fair rock	Moderate rock-fall susceptibility
10–40	Good rock	Low rock-fall susceptibility
40–100	Very good rock	Low rock-fall susceptibility

and coarser material believed to have been deposited by larger streams than those that form alluvial fans with less steep slopes.

Alluvium—Stream-channel and flood-plain sediment along the canyon bottom deposited by the American Fork River. Sediment includes clay, silt, sand, and rounded-to-subangular pebble-to boulder-sized clasts. See figure 10L for example. Locally includes angular rocks that range up to boulder size that were derived from rock falls from limestone cliffs adjacent to the river.

ML—Modified land, primarily fill material beneath Highway 92.

Rock-Mass Quality

Results from Rock-Mass-Quality measurements are given in Appendix A. All measurement locations are shown on plate 1. Photographs of some of the measurement locations with various Q values are shown in Appendix B. Q values range from 0.11 to 16.96 (Appendixes A and B). The distribution of Q values is as follows: 71 percent are between 0.1 and 1, 22 percent are between 1 and 4, 6 percent are between 4 and 10, and 1 percent are between 10 and 40. Results from previous Rock-Mass-Quality assessments by Barton and others (1974) and Harp and Jibson (2002) are helpful for classifying and interpreting these values. Table 4 contains a comparison of the descriptive classification schemes used by these previous studies. According to these classification schemes, 71 percent of our measurement locations are classified as having high rock-fall susceptibility and very poor rock, 28 percent are classified as moderate

susceptibility and poor to fair rock, and 1 percent are classified as low susceptibility and good rock.

In order to use our measured Q values in map form, we grouped them in accordance with our field observations, that is, our observation that rock-fall frequency is correlated with the steepness of rock bedding planes. Table 5 shows average Q values and the associated standard deviations when measured Q values shown in Appendix A are grouped according to the type of bedrock map unit (that is, steeply dipping, moderately dipping, and shallow dipping bedrock, pl. 1). Average Q values show a negative correlation with steepness of dip (table 5), which agrees with our field observations. That is, as dip increases, average Q values decrease. The separation between average Q values for each bedrock category is about 0.6. The standard deviation results (table 5) show that within any unit there are a wide range of Q values, but that this range becomes narrower as bedrock dip becomes steeper.

Other useful parameters that can be derived from Rock-Mass-Quality measurements include estimates of relative and absolute block size, apparent shear strength, and relative “tightness” of discontinuities. Results from block size and volume estimates vary somewhat in magnitude depending on the technique used, but consistently show that on average, blocks increase in size as bedrock dip decreases (table 5). However, all block volume and size estimates should be thought of as indicators of general trends, and not necessarily indicators of extreme values. Field observations indicated that block sizes can vary greatly over short distances. We observed very large blocks (up to about 165 m³) throughout the campground and downslope from both shallow, moderate, and steeply dipping bedrock.

Table 5. Rock Mass Quality data compiled according to bedrock map units shown on plate 1.

Map Unit	Number of Rock Mass Quality field measurements	Average Q value	Standard deviation of Q values	Average relative block size (non-dimensional)	Standard deviation of relative block sizes (non-dimensional)	Average absolute block volume (cm ³)	Standard deviation of absolute block volumes (cm ³)	Average absolute block size (edge length, cm)	Standard deviation of absolute block sizes (cm)	Average Apparent shear strength (friction angle, degrees)	Standard deviation of apparent shear strength values (degrees)	Average relative rock "tightness"	Standard deviation of rock "tightness" values
Shallow dipping bedrock	22	1.86	3.56	2.16	3.16	5137	11056	12.9	7.9	64	6	0.39	0.19
Moderately dipping bedrock or fold axial zone	25	1.20	1.50	1.61	1.60	4247	7889	12.5	7.2	63	7	0.32	0.14
Steeply dipping bedrock	25	0.57	0.55	1.25	0.87	1862	1905	11.1	3.8	58	8	0.25	0.11



A



B



C



D



E

Figure 11. Examples of Extreme Runout (ER) measurement sites. Locations measured are shown with an arrow. (A) Site ER9. Photograph taken October 28, 2004. (B) Site ER11. Footslope is in the upper part of the photograph. Photograph taken October 25, 2004. (C) Site ER13. Photograph taken October 25, 2004. (D) Site ER15. Distance measured from north and south footslopes. Photograph taken October 25, 2004. (E) Site ER 25. Photograph taken October 28, 2004.

Table 6. Data from Extreme Runout measurements.

Site Name	Measured Distance (m)	Block Size (m ³)	Comments
ER1	15	6.0	At Campsite 14
ER2	13.5	7.9	Just east of Comfort station 2, on south side of campground road across from campsite 21.
ER3	11	0.1	Near campsite 5
ER4	8	30.0	Near campsite 7
ER5	18.5	4.8	Single boulder from north slope, between Hwy 92 and Campsites 2 and 3
ER6	10.5	3.8	Between Campsites 26 and 30
ER7	16.2	3.9	At Campsite 32
ER8	15.5	0.7	Deposited on debris fan near comfort station 4
ER9	19.9	11.2	December 2000 rockfall ~ 500 ft west of campground entrance
ER10	19.5	20.4	At Grey Cliffs picnic area, near 2nd picnic pad from west end
ER11	14.5	<0.1	At Grey Cliffs picnic area, between 6th and 7th pads from west end
ER12	14	16.9	At Grey Cliffs picnic area, near 7th pad from west end
ER13	17.5	4.8	At Grey Cliffs picnic area, between 8th and 9th pads from west end
ER14	18	22.8	At Grey Cliffs picnic area, between 9th and 10th pads from west end
ER15	38	125.0	In North Mill, 38 m from north footslope, 36 m from south footslope
ER16	17.5	165.0	At Campsite 42

Table 6. Data from Extreme Runout measurements—Continued.

ER17	23.3	175.0	Single boulder (House Rock) east of Timpanogos Monument
ER18	31	5.8	Single boulder at entrance to Swinging Bridge picnic area
ER19	16	3.7	Single boulder in Timpanogos Admin office yard
ER20	16	0.5	Fresh (week of 10/25/04) rockfall just west of campsite 79, divot in campground road, boulder in creek.
ER21	7	7.4	Single boulder in river downslope from Campsite 6
ER22	19	24.0	Single boulder on north side of river at North Mill Group Campsite
ER23	35	7.9	Single boulder in river between Campsites 29 and 32
ER24	7.5	0.2	Rockfall deposit just east of Campsite 63
ER25	12	7.5	Rockfall deposit just west of Campsite 68
ER26	10.5	<0.1	Single boulder, near others from different falls, near east end of Campsite 79

Table 7. Data from Distribution of rock-fall Runout measurements. Numbers that are bold and italicized were estimated from regression equations shown in figure 13.

Site Name						
Distance from footslope (m)	DR1 (number of rocks counted)	DR2 (number of rocks counted)	DR3 (number of rocks counted)	DR4 (number of rocks counted)	DR5 (number of rocks counted)	DR6 (number of rocks counted)
0–5	60	160	99	68	214	112
5–10	61	100	59	31	74	55
10–15	48	90	19	21	15	8
15–20	60	26	14	10	31	3
20–25	6	28	6	1	19	1
25–30	6	7	3	1	5	0
30–35	5	5	2	0	3	0
35–40	3	3	1	0	2	0
40–45	2	2	0	0	1	0
45–50	1	1	0	0	0	0
50–55	0	0	0	0	0	0
Total (0–55)	252	422	203	132	364	179



A

Figure 12. Examples of the sites where the distribution of rock-fall runout (DR) was measured. (A) Site DR1 at campsite 42. Photograph taken October 25, 2004. (B) Site DR3 in Grey Cliffs picnic area. Photograph taken November 14, 2004. (C) Site DR5 at campsite 35. Photograph taken November 14, 2004.



B



C

Estimates of relative block sizes (the relative length of a block edge) range from 0.16 (Q43, Appendix A) to 14.13 (Q17, Appendix A). These values indicate that location Q17 has block sizes that are about 88 times larger than blocks at site Q43. Relative block sizes vary systematically according to bedrock map unit (table 5). Shallow-dipping bedrock has the largest average relative block size (2.2, table 5), and steeply dipping bedrock has the smallest average block size (1.3, table 5). These data indicate that, on average, blocks from shallow-dipping bedrock are roughly two times larger than blocks in steeply dipping bedrock.

Estimates of absolute block volume (V_b , in cm^3) range from 50 cm^3 (Q8 Appendix A) to $50,000 \text{ cm}^3$ (Q13, Appendix A). Absolute block volumes also vary systematically according to map unit (table 5). Shallow-dipping bedrock has the largest average V_b (5137 cm^3 , table 5), and steeply dipping bedrock has the smallest average V_b (1862 cm^3 , table 5). These data indicated that, on average, blocks in shallow-dipping bedrock are roughly three times larger than blocks in steeply-dipping bedrock. Absolute block sizes derived using $\sqrt[3]{V_b}$ range from 4 cm (Q8 and Q45, Appendix A) to 37 cm (Q13, Appendix A). These also vary systematically according to bedrock dip with the largest average sizes in shallow-dipping bedrock (12.9 cm, table 5) and the smallest in steeply dipping bedrock (11.1 cm, table 5).

Apparent shear strength data derived from our measurements and expressed as a total friction angle are given in Appendix A. Angles range from 45° (5 sites, Appendix A) to 72° (9 sites, Appendix A). Average angles compiled for each bedrock unit (table 5), vary systematically, with shallow-dipping bedrock having the largest angles (64°), and steeply dipping bedrock having the smallest angles (58°).

Relative rock “tightness” data derived from our measurements are given in Appendix A. “Tightness” values range from 0.11 (Q61, Appendix A) to 0.80 (Q65 and Q66, Appendix A). Average values compiled for each bedrock unit (table 5), vary systematically with shallow-dipping bedrock having the “tightest” rock (0.19, table 5) and steeply dipping bedrock having the “loosest” rock (0.11).

In summary, all data indicate that, in general, as bedrock dip increases, Q , block size, shear strength, and rock “tightness” all decrease. However, all of these parameters can vary widely within each bedrock map unit.

Rock-Fall Runout

Results from measurements of extreme runout distances (ER) and the distribution of distances at clusters of rocks (DR) are given in tables 6 and 7, respectively.

Footslope locations where the distances were measured are shown on plate 1. Examples of measurement sites are shown on figures 11 and 12. Extreme runout distances range from 7 m to 38 m (table 6) and average about 17 m. The 38-m measurement was made at a 125 m^3 rock in the North Mill group campsite (fig. 11D). The south edge of this rock was 38 m from the north footslope, and the north edge was 36 m from the south footslope.

We are not sure if this rock originated on the north or south slope, but we suspect it came from the north slope because it would not have had to cross the river to get to its current location. The location of this rock clearly illustrates that large rocks from previous rock falls have traveled to the center of the canyon. The widest part of the canyon bottom at Little Mill campground is only about 80 m, with the center located about 40 m from each footslope. Therefore, the location of this rock also illustrates that rocks from future rock falls are capable of traveling to the center of the canyon, and that *all locations in the canyon at Little Mill are exposed to hazards from falling rocks*. Given this fact, and the fact that all campsites are located along the canyon floor, the next reasonable question to ask is: What is the likelihood of rocks traveling given distances across the canyon floor? In order to answer this question, we measured the distribution of distances at clusters of rocks from previous rock falls. Our goal in making these measurements was to estimate the percentage of the total number of rocks (in each individual cluster) that traveled given distances across the canyon floor. When evaluating these estimates, the reader should keep in mind that many rocks never make it to the canyon floor—they come to rest on the hillslope itself. Our percentage estimates, therefore, are based on the total number of rocks that travel past the footslope, not the total number of rocks that fall.

Results from the distribution of distances at clusters of rocks (DR, pl. 1) are given in table 7. The number of rocks counted in 5 m intervals at each site are shown graphically in figure 13. Because rocks became difficult, and sometimes impossible, to count in some areas far from the footslope, the number of rocks in these areas were estimated by finding a best fit line to the available data using a least squares regression analysis. The equations for the best-fit lines at each site are given in figure 13. The number of rocks estimated using these equations are shown in bold, italicized type in table 7. Once the number of rocks were available for all distance intervals, they were converted to percentages of the total of rocks at each site (fig. 14). Figure 14 shows a negative correlation between distance from the footslope and the percent of rocks. Said another way, as the distance from the footslope increases, the number of rocks decreases. Furthermore, this relation is exponential, with more than 89 percent of rocks located within 20 m of the footslope. The number of rocks that traveled past 20 m ranged from about 1 percent at site DR6 to about 11 percent at site DR2 (fig. 14). These percentages can be used to estimate the number of rocks expected at various distances from future rock falls. For example, taking a conservative approach (from a hazard perspective) and by using the highest percentage of rocks at each distance, indicates that for rocks that travel beyond the footslope, about 76 percent will travel beyond 5 m, 52 percent will travel beyond 10 m, 33 percent will travel beyond 15 m, 11 percent will travel beyond 20 m, 7 percent beyond 25 m, and 4 percent will travel beyond 30 m. These percentages could be used in a risk assessment based on distance from the footslope.

We did not observe a correlation between runout and steepness of bedrock dip, but we expect a positive correlation between

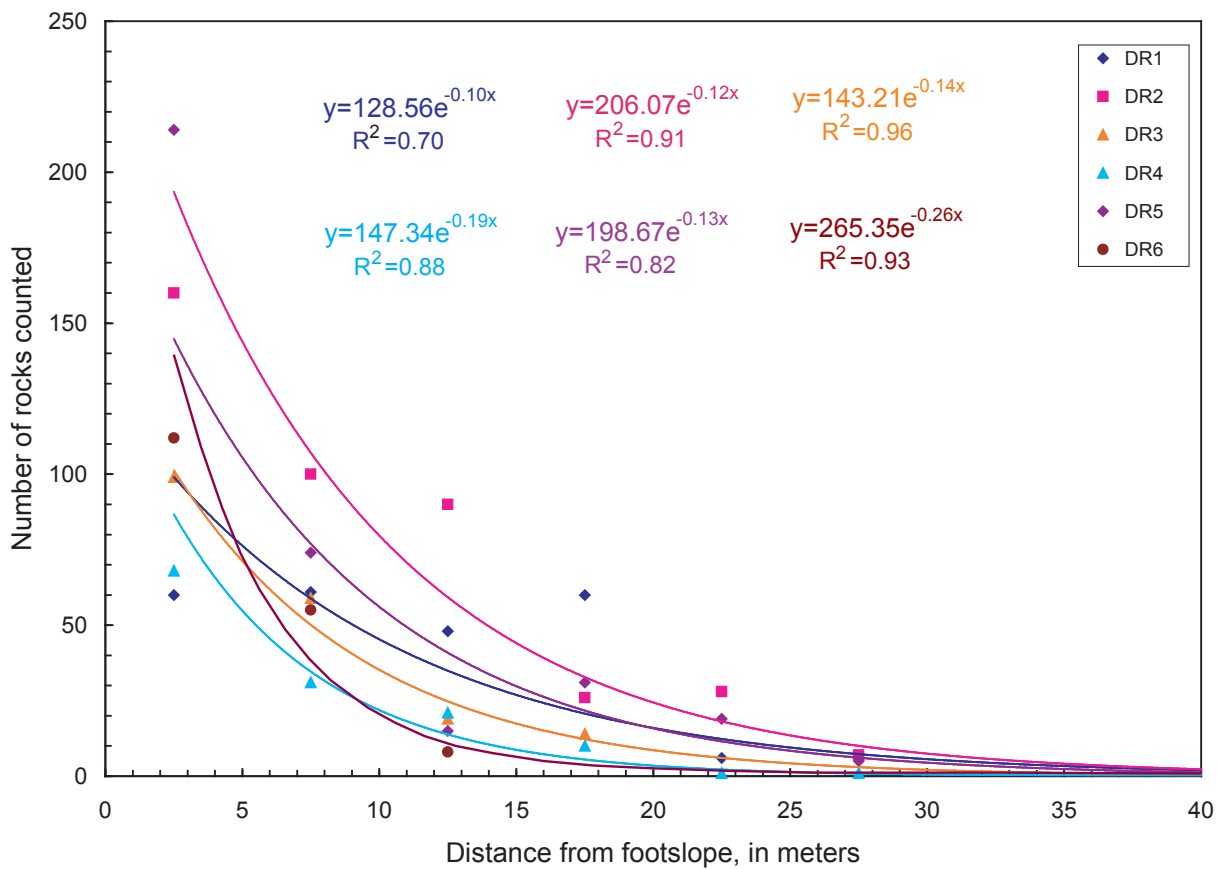


Figure 13. Diagram showing numbers of rocks counted with respect to distances from the footslope at DR locations (see pl. 1). At locations far from the footslope where rocks could not be counted, counts were estimated using the regression equations shown (see table 7 and text for additional explanation).

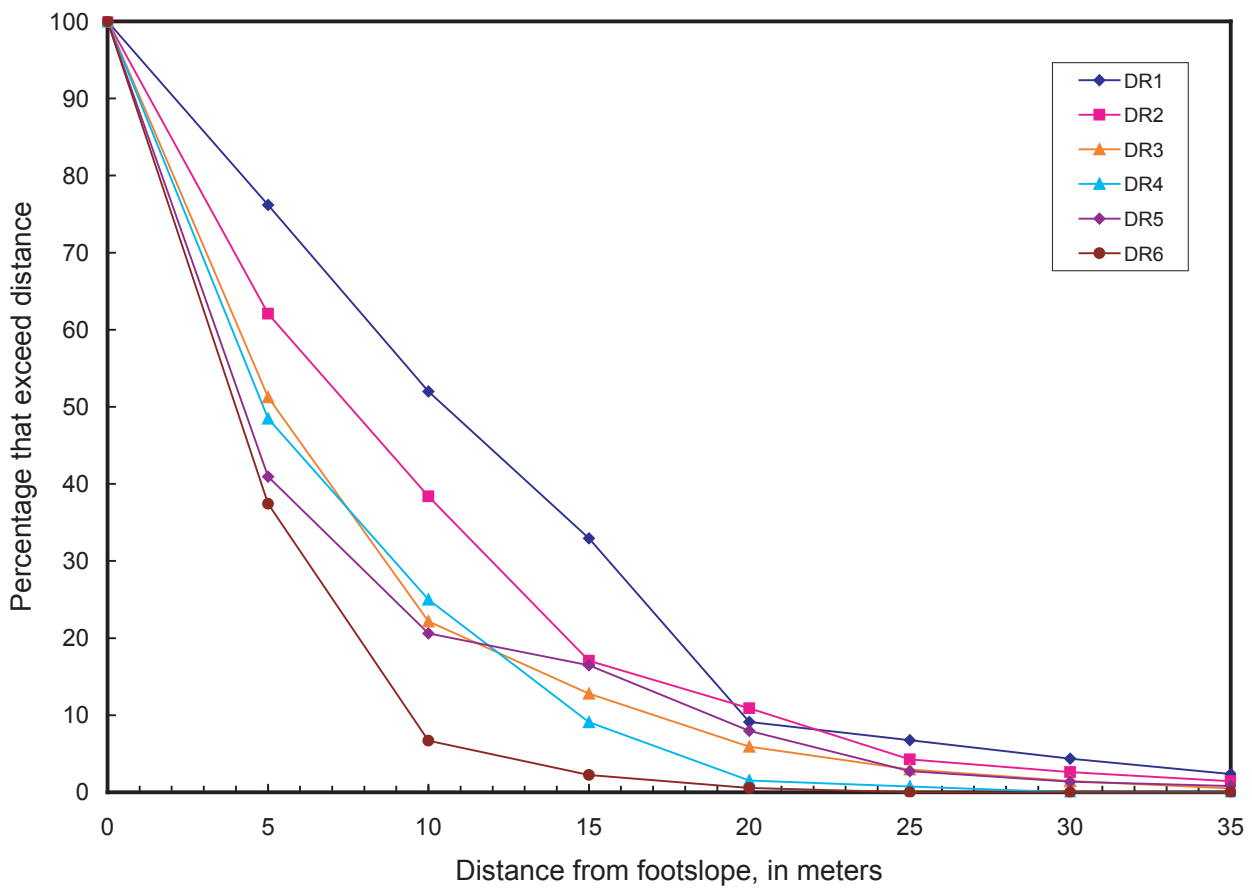


Figure 14. Diagram showing the percent of total rocks counted with respect to distances from the footslope at DR locations (see pl. 1 and table 7).

runout and the amount of topographic relief above different parts of the canyon floor. Additionally, other factors that control runout distance are the shape of the rocks, the starting points of rock falls, the steepness, roughness, and hardness of rock-fall travel paths, and the number and density of obstacles (for example, vegetation or large rocks from previous rock falls) within rock-fall travel paths. An analysis of all of these factors currently is beyond the scope of this investigation, primarily because high-resolution topographic data required for large-scale rock-fall modeling currently are unavailable.

Hazard Interpretation

The results described above are interpreted in the form of a rock-fall hazard map on plate 2. Rock-fall initiation, travel paths, and deposition zones are interpreted using a multiple-level, relative-hazard classification scheme. The three levels of susceptibility for rock-fall initiation are very high, high, and moderate. These levels directly correspond with steep-, moderate-, and shallow-dipping bedrock units shown on plate 1. Average Q values given in table 5 support this interpretation. The average Q value of 0.57 for steeply dipping rocks ranks as highly susceptible rock according to Harp and Jibson (2002) and very poor rock according to Barton and others (1974). We chose to use the “very-high susceptibility” label for steeply dipping rocks because of the repeated history of rock-fall events, the extreme relief, and fresh talus deposits that generally are found in these areas. At the opposite end of the susceptibility ranking is the “moderate” label, which corresponds to shallow-dipping bedrock. The average Q value of 1.86 for shallow-dipping bedrock ranks as moderately susceptible rock according to Harp and Jibson (2002) and poor rock according to Barton and others (1974). We

chose the “moderate”, rather than a “low” susceptibility label because of these previous guidelines, as well as the fact that some historical rock falls initiated from shallow-dipping bedrock. There was significant relief and fresh talus in some of these areas. In general, our hazard ranking corresponds to the relative frequency of rock fall initiation, with “very high” areas having the highest frequency of initiation and “moderate” areas having the lowest frequency.

Potential travel paths downslope from initiation zones are divided into three classes labeled primary, secondary, and ternary. These classes respectively correspond with (1) young talus; (2) older talus, colluvium, soil, and debris cones; and (3) debris fans. In general, these classes correspond to the relative frequency of a rock traveling down a specific path, with primary paths experiencing the highest frequency of rocks and ternary paths having the lowest frequency. Debris cones are included in the secondary travel path class because they generally are steeper than debris fans and, therefore, would probably not significantly slow the velocity of moving rocks. Debris fans primarily are debris-flow deposition zones. In areas where falling rocks impact debris fans, many rocks come to rest near the heads of the fans. However, some rocks moving at high velocities may travel down fan surfaces. We, therefore, classify all fans as ternary travel paths.

Most rocks moving down travel paths probably would be rolling or bouncing when they cross the footslope line and enter the campground. Some small rocks (fist sized or less as defined by Wieczorek and Snyder, 1999) may also be “fly rock”, that is, airborne rock fragments that result from the impact of larger rocks on cliff or talus areas. Bouncing is included as an expected form of movement in spite of the fact that previous work by Ritchie (1963) indicated that rocks moving down slopes less than about 45 degrees would predominantly be rolling (fig. 15). The slopes of most travel paths immediately upslope from the campground are less than about 45°. Our experience in other geographic areas indicates that boulders can bounce on nearly flat slopes for hundreds of meters depending on their momentum, shape, and the nature of the substrate. Historical rock fall number 6 (table 3), as well as scars in the campground road (fig. 8), indicate that some rocks bounce through the campground. In areas of the campground that lie immediately below bedrock cliffs, such as campsite 33 (pl. 2), rocks would be bouncing or falling as they move downslope (fig. 15).

The likely deposition zones for rocks that travel beyond the footslope are shown as rock-fall runout zones on plate 2. These zones are mapped as alluvium and modified land on plate 1. Rock-fall runout is portrayed by variably colored lines that show the distances from the north and south footslopes in 10 m increments. We do not show these lines in areas downslope from debris fans because the predominant transport and depositional processes that operate on these fans is debris flow, not rock fall. As described in the results section, rocks that travel past the 10, 20, and 30 m runout lines are roughly equal to 52, 11, and 4 percent of all rocks that travel past the footslope. These numbers would be lower if they were expressed as the percentage

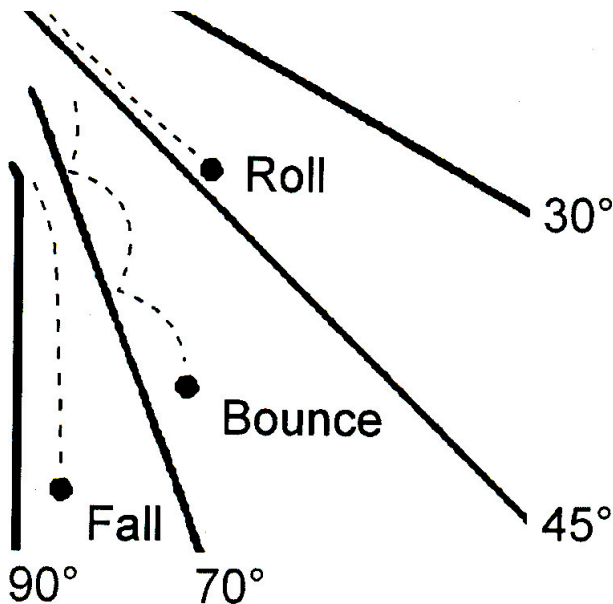


Figure 15. Diagram showing the likely movement of rocks as a function of slope angle (from Dorren, 2003; modified from Ritchie, 1963).

Table 8. Rock-fall hazard at individual campsites.

Susceptibility/travel path	Campsites downslope (Numbers, total number of sites in brackets)	Campsites where distance to footslope is < 10 m	Campsites where distance to footslope is between 10 and 20 m	Campsites where distance to footslope is between 20 and 30 m	Campsites where distance to footslope is > 30 m
Very High Susceptibility with Primary Travel Path	2-7, 9-21 [19]	5-7, 9, 12-14, 19 [8]	2-3, 10, 11, 15 [5]	4, 16, 18, 21 [4]	17, 20 [2]
Very High Susceptibility with Secondary Travel Path	1 [1]	None	None	1 [1]	None
High Susceptibility with Primary Travel Path	30, 33, 68-70, 78, 79 [7]	30, 33, 68-70, 78, 79 [7]	None	None	None
High Susceptibility with Secondary Travel Path	25, 26, 29, 31 [4]	25, 26, 31 [3]	None	29 [1]	None
Moderate Susceptibility with Primary Travel Path	32, 34-38, 41-43, 45, 47, 48, 50, 51, 52, 63-67 [20]	34-38, 41-43, 48, 63, 64 [11]	32, 45, 47, 67 [4]	50, 65-66 [3]	51, 52 [2]
Moderate Susceptibility with Secondary Travel Path	40, 44, 46, 49, 53-62, 71-74, 75, 76, 77 [21]	40, 44, 49, 61, 62, 71-74, 75-77 [12]	46, 53, 54, 57, 58 [5]	60 [1]	55, 56, 59 [3]
Low Susceptibility on periphery of large debris fans	8, 22, 23, 24, 27, 28, 39 [7]	Not Applicable	Not Applicable	Not Applicable	Not Applicable

of all rocks that fall (including those that stay upslope from the footslope). Unfortunately, we do not have a good estimate of the total number of rocks that fall over a given period of time and, therefore, cannot express the percentages in this manner.

The location of individual campsites with respect to initiation susceptibility, travel paths, and runout lines is graphically shown on plate 2 and presented in tabular form in table 8. Thirty-one of the seventy-nine campsites are downslope from very high or high rock-fall susceptibility zones (table 8). Of these, eighteen are located within 10 m of the footslope, five are between 10 and 20 m, six are between 20 and 30 m, and two are greater than 30 m. Forty-one campsites are downslope from moderate susceptibility zones. Of these, twenty-three are located within 10 m of the footslope, nine are between 10 and 20 m, four are between 20 and 30 m, and five are greater than 30 m. Seven campsites are located around the downslope periphery of debris fans and are shown as having low susceptibility to rock-fall hazards. We assign a low-susceptibility ranking because they are partially shielded from falling rocks by the fans. These sites are, however, susceptible to debris-flow hazards. Cannon (1985) and Wieczorek and others (1989) describe examples of recent debris flows in the Wasatch Range. A specific example of a debris flow in the immediate vicinity of Little Mill campground occurred in June 1983 and impacted the debris fan at the mouth of Tank Canyon (fig. 1B), located about 1 km west of the west entrance to Little Mill (October 2004, personal communication with John Hendrix and Dean Larsen, USFS). This debris flow covered the fan with mud, boulders, and woody debris.

Need for Rock-Fall Modeling

A dynamic analysis of rock-fall behavior at Little Mill would be useful to better estimate rock-fall motion and runout at specific campsites, and to provide constraints for the design of mitigation schemes. Rock-fall behavior is a function of topography (for example, slope angle and length), the size and shape of falling rocks, materials along travel paths, and the number and density of obstacles (for example, vegetation) within travel paths. These factors could be taken into account in a dynamic analysis of rock fall, using currently available rock-fall modeling software (for example, CRSP, Colorado Rock Fall Simulation Software, Jones and others, 2000; STONE, Guzzetti and others, 2002). The first step in conducting such an analysis would be the collection of detailed topographic information (probably in the form of profiles at specific sites) that could be used as a basic modeling parameter. This information could be collected using field surveying techniques or possibly from existing aerial photographs using photogrammetric techniques. Information on the other factors could be estimated from field observations. Historical rock-fall sites should be used as ground truth for such a modeling effort.

Conclusions

All campsites within Little Mill campground are exposed to hazards from falling rocks. The hazard is highest in areas close

to the margins of the canyon floor and lowest in the center of the canyon. In general, rock-fall frequency and rock-mass quality vary systematically according to the level of deformation of cliff-forming, limestone bedrock upslope from the campground. Rock falls occur most frequently from areas of steeply dipping bedrock, and least frequently from areas of shallow-dipping bedrock. Hazard mapping shows that, of the seventy-nine campsites at Little Mill, thirty one are located downslope from very high or high rock-fall susceptibility areas, forty one are downslope from moderate susceptibility areas, and seven are located around the periphery of debris fans, and thus have a low rock-fall hazard ranking. Distances from the margins of the canyon floor (the footslopes of the canyon walls) to individual campsites provide a basis for evaluating rock-fall hazard at each site. Measurements of rock travel distances of previous rock falls indicate that, of the rocks that travel past the footslope (the downslope extent of talus deposits), about 52 percent go beyond 10 m, 11 percent go beyond 20 m, and 4 percent go beyond 30 m. Rock-fall modeling would better define rock-fall motion and travel distances at individual sites.

Acknowledgements

We are grateful to Jonathan Godt and Gerry Wieczorek for their constructive reviews of this report and to Margo Johnson, who prepared and edited the final report and plates.

References

- Baker, A.A., and Crittenden, M.D., Jr., 1961, Geology of the Timpanogos Cave quadrangle, Utah: U.S. Geological Survey Geologic Quadrangle GQ-132, 1:24,000 scale.
- Barton, Nick, Lien, R., and Lunde, J., 1974, Engineering classification of rock masses for the design of tunnel support: Norwegian Geotechnical Institute, Oslo, Norway, 48 p.
- Bates R.L., and Jackson, J.A., 1987, editors, Glossary of Geology (3rd 1987 edition): American Geological Institute, Alexandria Virginia, 788 p.
- Cannon, S.H., 1985, The lag rate and the travel-distance potential of debris flows, Masters Thesis, University of Colorado, Boulder, Colo., 141 p.
- Deere, D.U., and Deere, D.W., 1989, Rock Quality Designation (RQD) after twenty years: Contract Report GL-89-1, U.S. Army Engineer Waterways Experiment Station, Vicksburg, Miss., 25 p.
- Deseret News, 1994, California woman dies after rock falls on her: Deseret News, Metro edition, July 26, 1994, p. B1.
- Deseret News, 1995, Falling rock claims teen in American Fork Canyon stream: Deseret News, Metro edition, July 30, 1995, p. B1.
- Deseret News, 1997, Victims' kin file claims against Forest Service: Deserete News, Metro edition, March 27, 1997.
- Deseret News, 2000, Falling rock hurts hiker in canyon: Deseret News, Utah edition, October 16, 2000, p. B3.

- Dorren, L.K.A., 2003, A review of rockfall mechanics and modeling approaches: *Progress in Physical Geography*, v. 27, p. 69–87.
- Evans, S.G., and Hungr, O., 1993, The assessment of rockfall hazard at the base of talus slopes: *Canadian Geotechnical Journal*, v. 30, p. 620–636.
- Guzzetti, F., Reichenbach, P., and Wieczorek, G.F., 2003, Rockfall hazard and risk assessment in the Yosemite Valley, California, USA: *Natural Hazards and Earth System Sciences*, v. 3, p. 491–503.
- Guzzetti, F., Crosta, G., Detti, R., and Agliardi, F., 2002, STONE: a computer program for the three dimensional simulation of rock falls: *Computers and Geosciences*, v. 28, no. 9, p. 1,079–1,093.
- Harp, E.L., and Noble, M.A., 1993, An engineering rock classification to evaluate seismic rock-fall susceptibility and its application to the Wasatch Front, *Bulletin of the Association of Engineering Geologists*, v. 30, p. 293–319.
- Harp, E.L., and Jibson, R.W., 2002, Anomalous concentrations of seismically triggered rock falls in Pacoima Canyon: Are they caused by highly susceptible slopes or local amplification of seismic shaking: *Bulletin of the Seismological Society of America*, v. 92, no. 8, p. 3,180–3,189.
- Jones, C.L., Higgins, J.D., and Andrew, R.D., 2000, Colorado rockfall simulation program, version 4.0: Colorado Department of Transportation, Denver, Colo., 127 p.
- Machette, M.N., Personius, S.F., and Nelson, A.R., 1992, Paleoseismology of the Wasatch Fault Zone: A summary of recent investigations, interpretations, and conclusions, *in* Gori, P.L., and Hays, W.W., eds., *Assessment of regional earthquake hazards and risk along the Wasatch Front, Utah*: U.S. Geological Survey Professional Paper 1500-A, p. A1–A71.
- Mazzoccola D., and Sciesa, E., 2000, Implementation and comparison of different methods for rockfall hazard assessment in the Italian Alps, *in* Bromhead E., Dixon, N., and Ibsen, M-L. eds., *Landslides in research, theory and practice*, Proceedings of the 8th International Symposium on Landslides, June 26–30, 2000, Cardiff, Wales, v. 2, Thomas Telford, London, p. 1,035–1,040.
- Palmström, A., 1982, The volumetric joint count—A useful and simple measure of the degree of jointing: Proceedings of the 4th Congress of the International Association of Engineering Geologists, New Delhi, India, p. 221–228.
- Palmström, A., 1995, A rock mass characterization system for rock engineering purposes, PhD thesis, Oslo University, Norway, 400 p.
www.rockmass.net/phd/maintext.html
- Pillmore, C.L., 1989, Geologic photogrammetry in the U.S. Geological Survey: *Photogrammetric Engineering and Remote Sensing*, v. 55, p. 1,185–1,189.
- Ritchie, A.M., 1963, Evaluation of rockfall and its control: Highway Research Record 17, Washington, D.C.: Highway Research Board, National Research Council, p. 13–28.
- Selby, M.J., 1993, *Hillslope materials and processes* (2nd edition): Oxford University Press, New York, 451 p.
- Wieczorek, G.F., Lips, E.W., Ellen, S.D., 1989, Debris flows and hyperconcentrated floods along the Wasatch Front, Utah, 1983 and 1984, *Bulletin of the Association of Engineering Geologists*, v. 26, p. 191–208.
- Wieczorek G.F., and Snyder J.B., 1999, Rock falls from Glacier Point above Camp Curry, Yosemite National Park, California: U.S. Geological Survey Open-File Report 99–385, 13 p.
- Wieczorek G.F., and Snyder, J.B., 2003, Historical rock falls in Yosemite National Park, California: U.S. Geological Survey Open-File Report 03-491, 10 p.

APPENDIX A

Appendix A. Rock Mass Quality data from in and near Little Mill campground. Note that when RQD is less than or equal to 10, a nominal value of 10 is shown in this table and used for RQD in Equation 1. See plate 1 for locations of measurement sites.

Site name	<i>J_v</i>	<i>J_n</i>	<i>J_r</i>	<i>J_a</i>	<i>AF</i>	RQD	Relative block size (Edge length)	Average absolute block volume (cm ³)	Average absolute block size (Edge length, cm)	Estimated shear strength (degrees)	"Rock tightness" (1/ <i>AF</i>)	Rock mass quality (Q)
Q1	22	14	3	1	2.5	42.4	3.03	4696	17	72	0.40	3.63
Q2	12	14	3	1	5	75.4	5.39	28935	31	72	0.20	3.23
Q3	24	14	3	1	1.5	35.8	2.56	3617	15	72	0.67	5.11
Q4	24	14	2.5	1	2.5	35.8	2.56	3617	15	68	0.40	2.56
Q5	52	14	1.5	1	3	10	0.71	356	7	56	0.33	0.36
Q6	76	17.5	1.5	1	3.5	10	0.57	114	5	56	0.29	0.24
Q7	52	17.5	1.75	1	4	10	0.57	356	7	60	0.25	0.25
Q8	100	17.5	1	1	4	10	0.57	50	4	45	0.25	0.14
Q9	20	14	1.5	1	7.5	49	3.50	6250	18	56	0.13	0.70
Q10	16	14	1.5	1	3	62.2	4.44	12207	23	56	0.33	2.22
Q11	38	14	2	1	2	10	0.71	911	10	63	0.50	0.71
Q12	24	13	2.5	1	4	35.8	2.75	3617	15	68	0.25	1.72

Site name	J_v	J_n	J_r	J_a	AF	RQD	Relative block size (Edge length)	Average absolute block volume (cm^3)	Average absolute block size (Edge length, cm)	Estimated shear strength (degrees)	"Rock tightness" ($1/AF$)	Rock mass quality (Q)
Q13	10	12	3	1	5	82	6.83	50000	37	72	0.20	4.10
Q14	24	17.5	2	1	2.5	35.8	2.05	3617	15	63	0.40	1.64
Q15	34	14	2.5	1	4	2.8	0.20	1272	11	68	0.25	0.13
Q16	21	17.5	1.25	1	2.5	45.7	2.61	5399	18	51	0.40	1.31
Q17	22	3	3	1	2.5	42.4	14.13	4696	17	72	0.40	16.96
Q18	26	14	3	1	4	29.2	2.09	2845	14	72	0.25	1.56
Q19	35	13	2	1	8	10	0.77	1166	11	63	0.13	0.19
Q20	61	17.5	1.25	1	3	10	0.57	220	6	51	0.33	0.24
Q21	55	17.5	1.25	1	3	10	0.57	301	7	51	0.33	0.24
Q22	58	14	1.25	1	2.5	10	0.71	256	6	51	0.40	0.36
Q23	32	14	1	1	3.5	9.4	0.67	1526	12	45	0.29	0.19
Q24	38	17.5	1	1	5	10	0.57	911	10	45	0.20	0.11
Q25	18	17.5	2	1	8	55.6	3.18	8573	21	63	0.13	0.79

Site name	<i>Jv</i>	<i>Jn</i>	<i>Jr</i>	<i>Ja</i>	<i>AF</i>	RQD	Relative block size (Edge length)	Average absolute block volume (cm ³)	Average absolute block size (Edge length, cm)	Estimated shear strength (degrees)	"Rock tightness" (1/ <i>AF</i>)	Rock mass quality (Q)
Q26	28	13	1.5	1	5.5	22.6	1.74	2278	13	56	0.18	0.47
Q27	31	14	1	1	5	12.7	0.91	1678	12	45	0.20	0.18
Q28	24	17.5	1.5	1	3	35.8	2.05	3617	15	56	0.33	1.02
Q29	50	17.5	1	1	3.5	10	0.57	400	7	45	0.29	0.16
Q30	42	14	1.25	1	5.5	10	0.71	675	9	51	0.18	0.16
Q31	22	15	1.5	1	7	42.4	2.83	4696	17	56	0.14	0.61
Q32	26	15	3	1	4	29.2	1.95	2845	14	72	0.25	1.46
Q33	24	13	1.5	1	2.5	35.8	2.75	3617	15	56	0.40	1.65
Q34	24	13	2.25	1	3	35.8	2.75	3617	15	66	0.33	2.07
Q35	36	14	2	1	4	10	0.71	1072	10	63	0.25	0.36
Q36	46	17.5	3	1	2.5	10	0.57	514	8	72	0.40	0.69
Q37	35	15	1.75	1	8	10	0.67	1166	11	60	0.13	0.15
Q38	48	17.5	2	1	7	10	0.57	452	8	63	0.14	0.16

Site name	<i>Jv</i>	<i>Jn</i>	<i>Jr</i>	<i>Ja</i>	<i>AF</i>	RQD	Relative block size (Edge length)	Average absolute block volume (cm ³)	Average absolute block size (Edge length, cm)	Estimated shear strength (degrees)	"Rock tightness" (1/ <i>AF</i>)	Rock mass quality (Q)
Q39	38	17.5	1.75	1	3.5	10	0.57	911	10	60	0.29	0.29
Q40	62	17.5	1.5	1	2.5	10	0.57	210	6	56	0.40	0.34
Q41	27	15	2	1	8	25.9	1.73	2540	14	63	0.13	0.43
Q42	49	15	1.5	1	2.5	10	0.67	425	8	56	0.40	0.40
Q43	34	17.5	3	1	2.25	2.8	0.16	1272	11	72	0.44	0.21
Q44	56	17.5	1.75	1	2.25	10	0.57	285	7	60	0.44	0.44
Q45	88	17.5	2	1	2.5	10	0.57	73	4	63	0.40	0.46
Q46	30	14	2.5	1	3.5	16	1.14	1852	12	68	0.29	0.82
Q47	61	17.5	1.5	1	2.25	10	0.57	220	6	56	0.44	0.38
Q48	27	14	2.5	1	3.5	25.9	1.85	2540	14	68	0.29	1.32
Q49	59	17.5	1.75	1	6	10	0.57	243	6	60	0.17	0.17
Q50	35	17.5	2.25	1	3.5	10	0.57	1166	11	66	0.29	0.37
Q51	29	17.5	2.25	1	2.5	19.3	1.10	2050	13	66	0.40	0.99

Site name	<i>Jv</i>	<i>Jn</i>	<i>Jr</i>	<i>Ja</i>	<i>AF</i>	RQD	Relative block size (Edge length)	Average absolute block volume (cm ³)	Average absolute block size (Edge length, cm)	Estimated shear strength (degrees)	"Rock tightness" (1/ <i>AF</i>)	Rock mass quality (Q)
Q52	67	17.5	2	1	3.5	10	0.57	166	6	63	0.29	0.33
Q53	32	17.5	2.25	1	4.5	9.4	0.54	1526	12	66	0.22	0.27
Q54	33	17.5	2.25	1	3.5	6.1	0.35	1391	11	66	0.29	0.22
Q55	12	14	2.25	1	2.5	75.4	5.39	28935	31	66	0.40	4.85
Q56	49	14	1.5	1	1.5	10	0.71	425	8	56	0.67	0.71
Q57	38	17.5	2.25	1	7	10	0.57	911	10	66	0.14	0.18
Q58	66	17.5	2	1	4.5	10	0.57	174	6	63	0.22	0.25
Q59	49	17.5	2	1	2.5	10	0.57	425	8	63	0.40	0.46
Q60	28	14	2.25	1	2.5	22.6	1.61	2278	13	66	0.40	1.45
Q61	46	17.5	2.25	1	9.5	10	0.57	514	8	66	0.11	0.14
Q62	42	17.5	2.25	1	1.5	10	0.57	675	9	66	0.67	0.86
Q63	14	14	2.25	1	2.5	68.8	4.91	18222	26	66	0.40	4.42
Q64	51	17.5	2.25	1	2.5	10	0.57	377	7	66	0.40	0.51

Site name	<i>J_v</i>	<i>J_n</i>	<i>J_r</i>	<i>J_a</i>	<i>AF</i>	RQD	Relative block size (Edge length)	Average absolute block volume (cm ³)	Average absolute block size (Edge length, cm)	Estimated shear strength (degrees)	"Rock tightness" (1/ <i>AF</i>)	Rock mass quality (Q)
Q65	45	17.5	2	1	1.25	10	0.57	549	8	63	0.80	0.91
Q66	52	17.5	2	1	1.25	10	0.57	356	7	63	0.80	0.91
Q67	29	17.5	2	1	1.5	19.3	1.10	2050	13	63	0.67	1.47
Q68	44	17.5	2	1	3.5	10	0.57	587	8	63	0.29	0.33
Q69	15	17.5	2.25	1	5	65.5	3.74	14815	25	66	0.20	1.68
Q70	37	17.5	2.25	1	7	10	0.57	987	10	66	0.14	0.18
Q71	24	17.5	2	1	8	35.8	2.05	3617	15	63	0.13	0.51
Q72	39	17.5	2.25	1	8.5	10	0.57	843	9	66	0.12	0.15

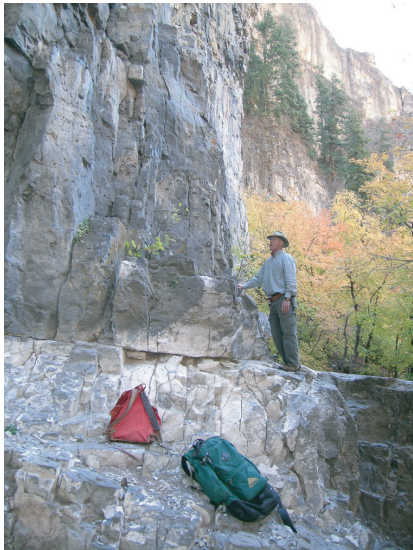
APPENDIX B



Q17, Q=16.96



Q13, Q=4.10



Q12, Q=1.72



Q67, Q=1.47



Q65, Q=0.91

Appendix B. Rock Mass Quality (Q) measurement locations. Photographs are individually labeled.



Q31, Q=0.61



Q26, Q=0.47



Q42, Q=0.40



Q35, Q=0.36



Q40, Q=0.34



Q53, Q=0.27



Q54, Q=0.22



Q=49, Q=0.17



Q29, Q=0.16



Q61, Q=0.14